ENGINEERING RESEARCH INSTITUTE
UNIVERSITY OF MICHIGAN
ANN ARBOR

THEORETICAL STUDY, DESIGN AND CONSTRUCTION OF C-W MAGNETRONS FOR FREQUENCY MODULATION

QUARTERLY PROGRESS REPORT NO. 3

Period Covering June 1, 1950 to September 1, 1950
Electron Tube Laboratory
Department of Electrical Engineering

BY

H. W. WELCH, JR.

J. R. BLACK
G. R. BREWER
J. S. NEEDLE
W. PETERSON
H. W. BATTEN
S. RUTHBERG

Approved By: W. G. Dow
G. Hok

Project M762

CONTRACT NO. W-36-039 sc-35561
SIGNAL CORPS, DEPARTMENT OF THE ARMY
DEPARTMENT OF ARMY PROJECT NO. 399-13-022
SIGNAL CORPS PROJECT NO. 112B-0

September, 1950

TABLE OF CONTENTS

PERSONNEL

Scientific and Engineering Personnel		*Time worked in man-months.
W. G. Dow	Prof. of Electrical Engineering	Supervisor
H. W. Welch	Research Physicist	1.54
J. R. Black	Research Engineer	2.51
G. Hok	Research Engineer	.60
J. S. Needle	Instructor of Electrical Engineering	.67
G. R. Brewer	Research Associate	2.57
S. Ruthberg	Research Associate	2.00
H. W. Batten	Research Assistant	.42
W. W. Peterson	Student Assistant	1.80

Service Personnel		
V. R. Burris	Machine Shop Foreman	1.58
R. F. Steiner	Assembly Technician	2.48
J. W. VanNatter	Assembly Technician	2.81
A. Town J. Mossar C. Pratt	Technicians	2.86
R. F. Denning T. G. Keith E. A. Kayser	Laboratory Machinists	4.94
M. J. Walker S. Spiegelman	Stenographers	1.70
N. Navarre	Draftsman	1.90

*Time worked is figured on the basis of 172 hours per month.

MAJOR REPORTS ISSUED TO DATE

Contract No. W-36-039 sc-32245. Subject: Theoretical Study, Design and Construction of C-W Magnetrons for Frequency Modulation.

Technical Report No. 1 --

H. W. Welch, Jr. "Space-Charge Effects and Frequency Characteristics of C-W Magnetrons Relative to the Problem of Frequency Modulation", November 15, 1948.

Technical Report No. 2 --

H. W. Welch, Jr., G. R. Brewer. "Operation of Interdigital Magnetrons in the Zero Order Mode", May 23, 1949.

Technical Report No. 3 --

H. W. Welch, Jr., J. R. Black, G. R. Brewer, G. Hok. "Final Report", May 27, 1949.

Contract No. W-36-039 sc-35561. Subject: Theoretical Study, Design and Construction of C-W Magnetrons for Frequency Modulation.

Interim Report --

H. W. Welch, Jr., J. R. Black, G. R. Brewer. December 15, 1949.

Quarterly Report No. 1 --

H. W. Welch, Jr., J. R. Black, G. R. Brewer, G. Hok, April, 1950.

Quarterly Report No. 2 --

H. W. Welch, Jr., J. R. Black, G. R. Brewer, J. S. Needle, W. Peterson, June, 1950.

LIST OF FIGURES

THEORETICAL STUDY, DESIGN AND CONSTRUCTION OF C-W MAGNETRONS FOR FREQUENCY MODULATION

QUARTERLY PROGRESS REPORT NO. 3

SEPTEMBER, 1950

1. OBJECTIVES FOR THE PERIOD (H. W. Welch, Jr.)

The purpose of this report is to summarize the progress in the University of Michigan Electron Tube Laboratory during the period from June 1, 1950, to September 1, 1950, on Contract No. W-36-039 sc-35561.

The general objectives of the program under this contract are to increase the knowledge of space charge effects and frequency characteristics in c-w magnetrons and apply this knowledge to the development of magnetrons which can be frequency-modulated. Prior to March 1, the emphasis had been on the2000-2400 Mc range. The general technique adopted for development was the use of the magnetron-type space charge as a reactance-varying element used in a reactance tube in the same vacuum envelope as the oscillator magnetron. Three models were under development using this principle.

The study of a new method of modulation was initiated on this contract on March 1. This method is essentially the utilization of the frequency pushing phenomena, or voltage tuning. It was discovered by Wilbur, of General Electric Laboratories, early in 1949, that under cer-

tain conditons very wide frequency pushing at uniform power levels is obtainable. The observed frequency shifts have been between 1.5 to 1 and 15 to 1, depending on loading, efficiency and cathode temperature. The frequencies are all below 1000 megacycles. The loading conditions on the tubes have, so far, been quite restrictive, consisting of a load attached directly to the terminals of the anode structure. The Q's are of the order of 10 or less. With a transmission line between the tube and the load it will be quite possible to obtain Q's of the same order in the line which will immediately lead to problems involving long line effect. The objective of the new program is to obtain sufficient understanding of this type of operation that it may be extended to microwave frequencies of 3000-4000 megacycles.

In summary, the status of work on this contract at the beginning of June was as follows:

(a) The study of modulation by the reactance tube method had been brought to a standstill by the problem of power leakage out the cathode of the modulator section of the Model 6 magnetron. Modulation data could only be obtained under special loading conditions. The oscillator section had performed satisfactorily in the absence of the modulator cathode. Five of the eight tubes constructed had been operated in the desired mode (14 cm). A second type of tube (Model 8) was under construction. Work on the third model (Model 5) had been postponed indefinitely since the first tube constructed showed little promise of success.

(b) A special diode magnetron had been designed to permit exploration of distributions in the static magnetron space charge swarm by means of an electron beam and fluorescent screen. This tube was under construction.

(c) Theoretical analysis of the r-f properties of the magnetron space-charge (extending that given in Technical Report No. 1)[1] had been carried out and experimental tubes for checking the results were under construction.

(d) The study of low Q operation of magnetrons was started including investigation of frequency pushing, maximum current boundary, and various factors affecting performance.

(e) A low power, external cavity magnetron had been designed and was under construction. This tube is intended for use in experimental study of low Q operation.

The primary objectives for the period covered by this report were the following:

(a) To continue the study of low Q operation along the lines discussed in Quarterly Report No. 2 by both theoretical and experimental means.

(b) To construct the low power tube designed during the last period for use in study of low Q operation.

(c) To obtain experimental measurements of properties of the magnetron space charge with a specially constructed resonant diode.

(d) To consider changes in the Model 6 design which would prevent the power loss to the modulator cathode from impairing operation.

(e) To complete construction of the Model 8 magnetron and of a tube for study of the static magnetron space charge.

This report is intended only to report on progress in construction of tubes and development of theory and design during the period. Previously issued reports listed on page iii should be consulted if further information is desired.

---

1 See list of reports on page iii.

2. INDUCED CURRENTS IN MAGNETRONS (H. W. Batten, W. Peterson)

It can be shown that the product of the induced current to any electrode and the scalar potential on that electrode represents the only electrical energy (with a time average different from zero) delivered to the terminal if the time rate of change of the vector potential is small compared to the electric field at each point in the interaction space. The general development of such an induced current theory is not available in the literature;[1] nevertheless, we will confine this development merely to the introduction of the following relation for the induced current in the k'th electrode of a vacuum tube when no electrons are arriving at the terminal and to the application of this formula to the determination of induced currents in a magnetron. The result is applied to a special case.

The induced current i_k in the k'th electrode for the case when no electrons are arriving at the terminal is

$$i_k = -\frac{d}{dt}\int \psi_k \, dq = -\frac{d}{dt}\int \psi_k \, \rho \, dv \qquad 2.1$$

where the integration is carried over the interaction space, and

ρ = the space charge density

q = the charge

dv = the volume element

ψ_k = a scalar function defined as unity on the k'th electrode, zero on all other electrodes, and satisfying Laplace's equation throughout the interaction space.

---

[1] For a one-electron theory see
Shockley, W., "Currents Induced by a Moving Charge", Journal App. Phys., Vol. 9, pp. 635-636, October, 1938.

or Ramo, S., "Currents Induced by Electron Motion", Proc. I.R.E. Vol. 27, pp. 584-585, September, 1939.

We hope to present a general induced current theory at a later date. In the meantime, equation 2.1 will be given without proof. A brief argument for its acceptance which appeals to the intuition might be carried through as follows.

The flux terminating on a conductor due to a unit charge at some point P is numerically equal to the potential at point P if unit potential is placed on the conductor in question, all other conductors are at zero potential, and the charge is removed from the space. If this reciprocity relation is accepted then 2.1 is evident since a distribution of charge in this case gives a flux terminating on the conductor of $\int \psi_k \, dq$, and the displacement current flowing into the conductor is merely the time derivative of this value. (Note that the minus sign in 2.1 indicates that we are taking the current as positive when it flows from the external circuit to the terminal.)

We assume now that we are dealing with a magnetron operating in the π mode. All space charge in the interaction space is moving synchronously with an angular velocity ω_f,[2] and there is no radial motion of the electrons. Then

$$\rho = (r, \theta, t) = \rho_o (r, \theta-\theta_1) \quad \text{where}$$

$$\theta_1 = \omega_f t$$

and

$$\rho_o = \rho \text{ for } t = 0.$$

Now we desire the fundamental component of the induced current to the k'th element.

---

[2] For convenience the space angle between adjacent anode segments is considered π units in this section.

$$I_{km} = \frac{-1}{\pi} \int_{-\pi}^{\pi} \sin \theta_1 \left[\frac{d}{dt} \int \psi_k \, dq \right] d\theta_1. \qquad 2.3$$

The instantaneous induced current i_k has been assumed anti-symmetric about t = 0. This involves no loss of generality for symmetric spokes.

Integrating equation 2.3 by parts gives

$$I_{km} = \frac{-\omega_f}{\pi} \int_{-\pi}^{\pi} \sin \theta_1 \left[\frac{d}{d\theta_1} \int \psi_k \, dq \right] d\theta_1$$

$$= \frac{-\omega_f}{\pi} \sin \theta_1 \int \psi_k \, dq \Big]_{-\pi}^{\pi} + \frac{\omega_f}{\pi} \int_{-\pi}^{\pi} \cos \theta_1 \left[\int \psi_k \, dq \right] d\theta_1$$

$$= \frac{\omega_f}{\pi} \int_{-\pi}^{\pi} \cos \theta_1 \left[\int \psi_k \, dq \right] d\theta_1. \qquad 2.4$$

Now ψ_k and ρ are periodic functions of θ and $(\theta-\theta_1)$ respectively so that they can be represented by Fourier expansions of the form

$$\psi_k = \sum_n A_n \cos n\theta, \quad \frac{\rho}{Q} = \sum_a B_a \cos \; a(\theta-\theta_1) \qquad 2.5$$

where the A's and B's depend on r only, and Q is the total charge in the interaction space.[3]

Taking L as the axial length of the magnetron interaction space we can write equation 2.1 in the form

$$i_k = -\frac{d}{dt} \iint \psi_k \, \rho \, L dr d\theta \qquad 2.6$$

Substituting the Fourier expansions into this expression gives

$$i_k = -LQ \frac{d}{dt} \sum_{n,a} \iint A_n B_a \cos (n\theta) \cos a (\theta-\theta_1) \, dr d\theta \qquad 2.7$$

---

[3] Note that ψ_k and ρ have been taken symmetric about $\theta = \theta_1 = 0$. This choice is necessary in view of the anti-symmetric assumption on i_k.

Since the A's and B's are independent of θ, all terms of this expression vanish for $a \neq n$. Therefore

$$i_k = -LQ \frac{d}{dt} \sum_n \int \cos (n\theta) \cos n(\theta-\theta_1)\, d\theta \int A_n B_n\, rdr \qquad 2.8$$

$$= -LQ\pi \frac{d}{dt} \sum_n \cos n\theta_1 \int A_n B_n\, rdr$$

since the integration is to be taken over all space and

$$\int_{-\pi}^{\pi} \cos (n\theta) \cos n(\theta-\theta_1)\, d\theta = \pi \cos n\theta_1. \qquad 2.9$$

Returning to equation 2.4 and substituting from 2.8,

$$I_{km} = \omega_f LQ \sum_n \int_{-\pi}^{\pi} \cos \theta_1 \cos n\theta_1 d\theta_1 \int A_n B_n\, rdr$$

$$= \omega_f LQ\pi \int A_1 B_1\, rdr. \qquad 2.10$$

This can be written

$$I_{km} = 4Qf \int \left(\frac{\pi A_1}{2}\right) (\pi B_1\, Lrdr). \qquad 2.11$$

This last form has a significant interpretation because $\frac{\pi A_1}{2} \leq 1$ and $\int \pi\, B_1\, Lrdr \leq 1$.[4] Thus $(4Qf)$ is the maximum r-f induced current obtainable. It is realized by a point charge Q rotating at the anode radius with extremely small spacing between anode segments.

$$\text{The factor } F = \int \left(\frac{\pi A_1}{2}\right) (\pi B_1\, Lrdr) \qquad 2.12$$

represents a sort of "figure of merit" for the induced current under these circumstances.

---

[4] This remains to be shown.

The problem now is to determine the nature of this factor F. Defining

$$R = \frac{R}{r_c} \quad , \quad R_a = \frac{r_a}{r_c} \quad , \tag{2.13}$$

and

$$F = L\, r_c^2 \int \frac{\pi A_1}{2} \cdot \pi B_1 R \, d R \tag{2.14}$$

where the integration is taken over the interaction space, A_1 can be readily determined. We proceed as follows. From equation 2.5 one has

$$\psi_k = \sum_n A_n \cos n\theta \tag{2.15}$$

It is assumed that ψ_k is of the form $\psi_k = X(\theta) \cdot B(R)$. This is substituted into the equation $\Delta 2\, \psi_k = 0$, subject to boundary condition imposed by the periodicity of the anode structure, with the following result.

$$\psi_k = \sum_n C_n \left(R^{N/2} - D_n R^{-nN/2} \right) \cos n\theta \tag{2.16}$$

Here the C's and D's are independent of R and θ, and N/2 is the number of pairs of anode segments.

Since we are interested in the induced current in the anode, ψ_k must vanish on the cathode. Thus

$$D_n = 1. \tag{2.17}$$

C_n can be determined by assuming some form for ψ_k between anode elements at the anode radius. Suppose we assume linear variation so that $\psi_k(\theta, r_a)$ has the form shown in Figure 2.1. This gives

$$C_n \left(R_a^{nN/2} - R_a^{-nN/2} \right) = \frac{1}{\pi} \int_{-\pi}^{\pi} \psi_k (\theta, r_a) \cos n\theta \, d\theta$$

$$= \frac{2}{\pi \alpha n^2} \sin \frac{n\pi}{2} \sin n\alpha \, . \tag{2.18}$$

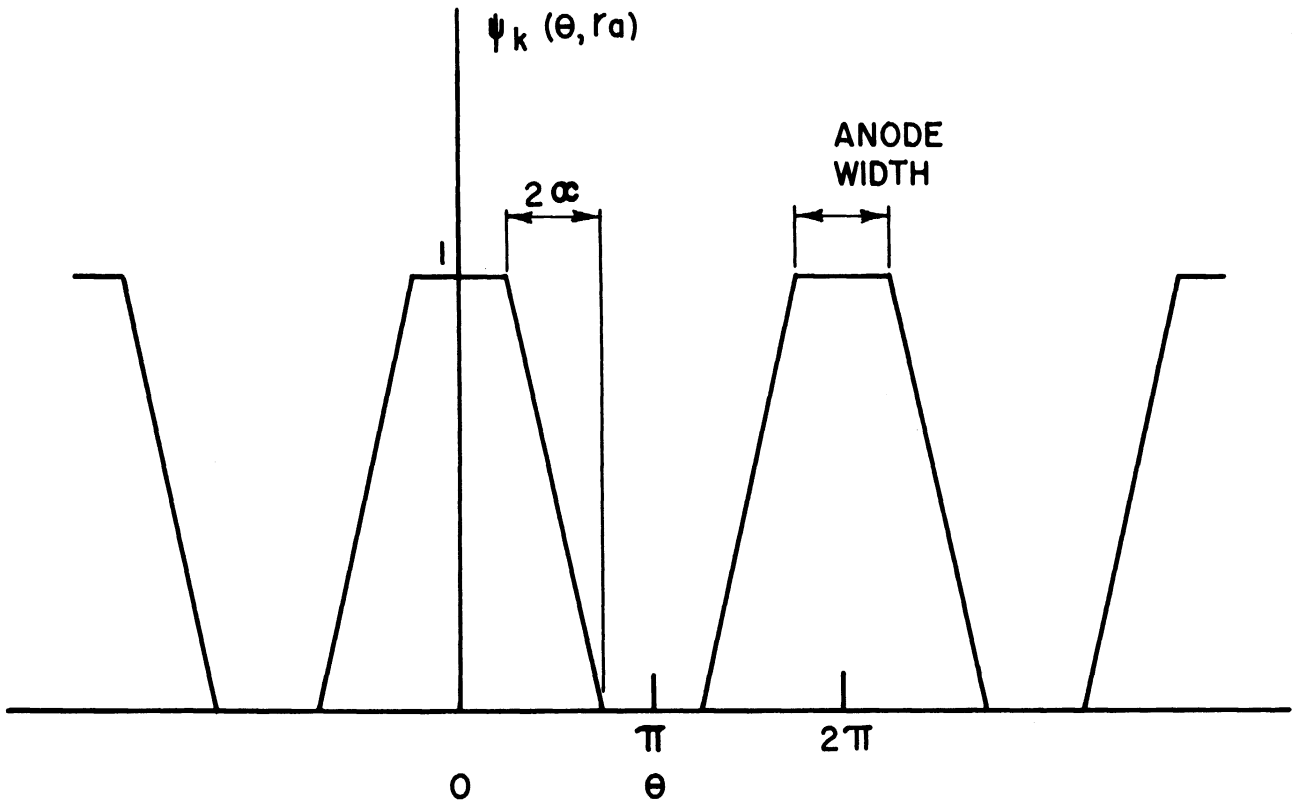

FIG. 2.1
ANGULAR VARIATION OF ψ_k AT ANODE RADIUS

From this we have

$$C_1 = \frac{1}{R_a^{N/2} - R_a^{-N/2}} \cdot \left(\frac{2}{\pi}\right) \left(\frac{\sin \alpha}{\alpha}\right) \qquad 2.19$$

and

$$A_1 = \frac{R^{N/2} - R^{-N/2}}{R_a^{N/2} - R_a^{-N/2}} \left(\frac{2}{\pi}\right) \left(\frac{\sin \alpha}{\alpha}\right). \qquad 2.20$$

The earlier observations concerning the factor $(\pi A_1/2)$ can easily be verified using this equation. Graphs of $(R^{N/2} - R^{-N/2})$ and $(\sin \alpha/\alpha)$ are given in Figures 2.2 and 2.3.

The determination of B_1, is not so easily carried through with the degree of rigor present in the solution for A_1 since the knowledge of the space-charge distribution in the interaction region is insufficient. However, we can obtain some insight into the magnetron behavior and some understanding of the space-charge swarm by assuming certain simple charge distributions and proceding to calculate B_1 and the induced current.

Consider a case in which the spokes have the well differentiated shape shown in Figure 2.4, and assume that within each spoke the space-charge density is a constant. Then, using equation 2.5

$$B_1 = \frac{1}{\pi Q} \int_{-\pi}^{\pi} \rho \cos \theta \; d\theta \qquad 2.21$$

$$= \frac{2\rho}{\pi Q} \sin \beta \qquad 2.22$$

$$= \frac{1}{r_2^2 - r_1^2} \left(\frac{2}{\pi L}\right) \frac{\sin \beta}{\beta} \qquad 2.23$$

since $Q = \rho\pi(r_2^2 - r_1^2) \; \frac{\beta L}{\pi}$. $\qquad 2.24$

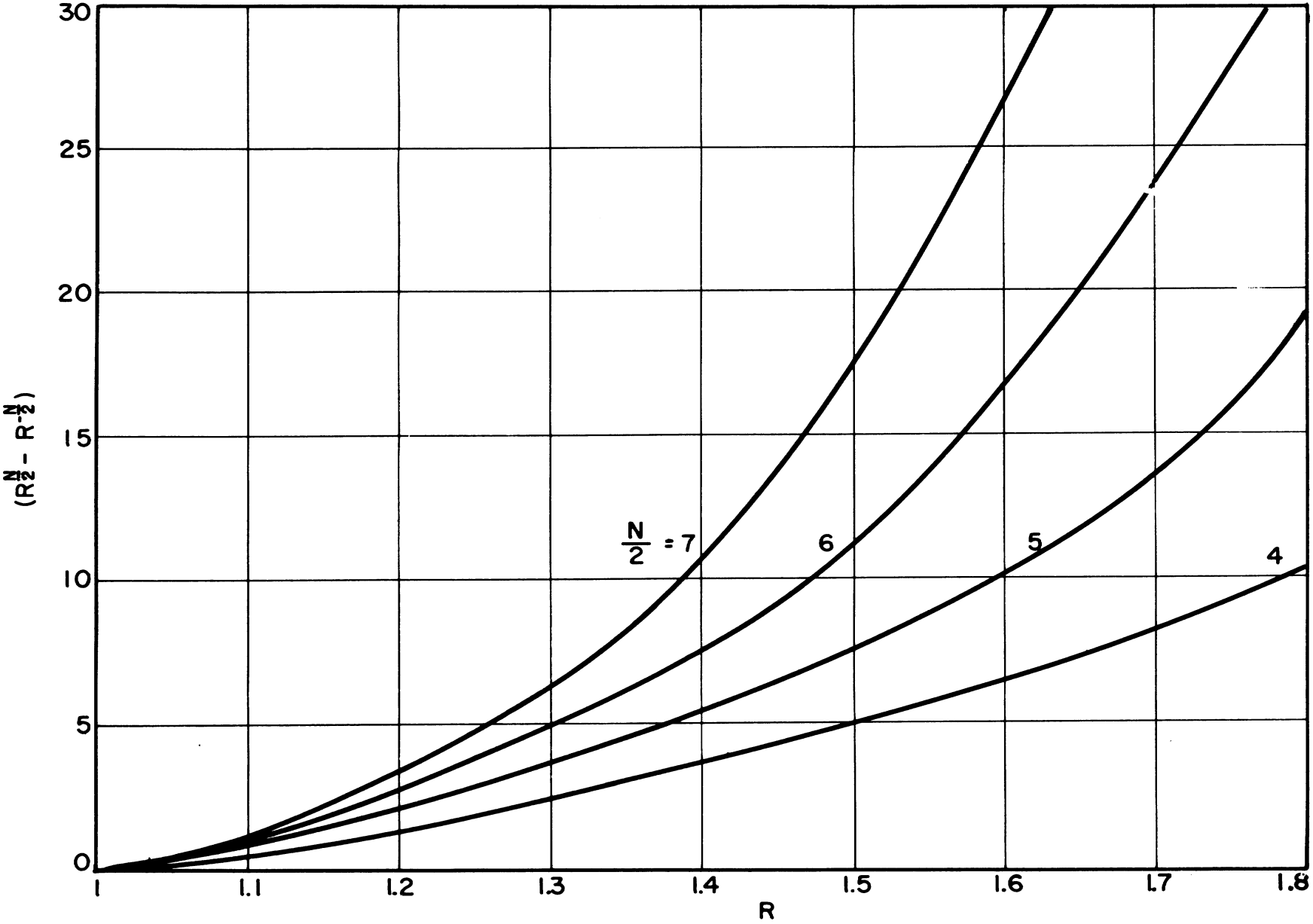

FIG. 2.2
FACTOR PRESENT IN EQUATION (2.20)

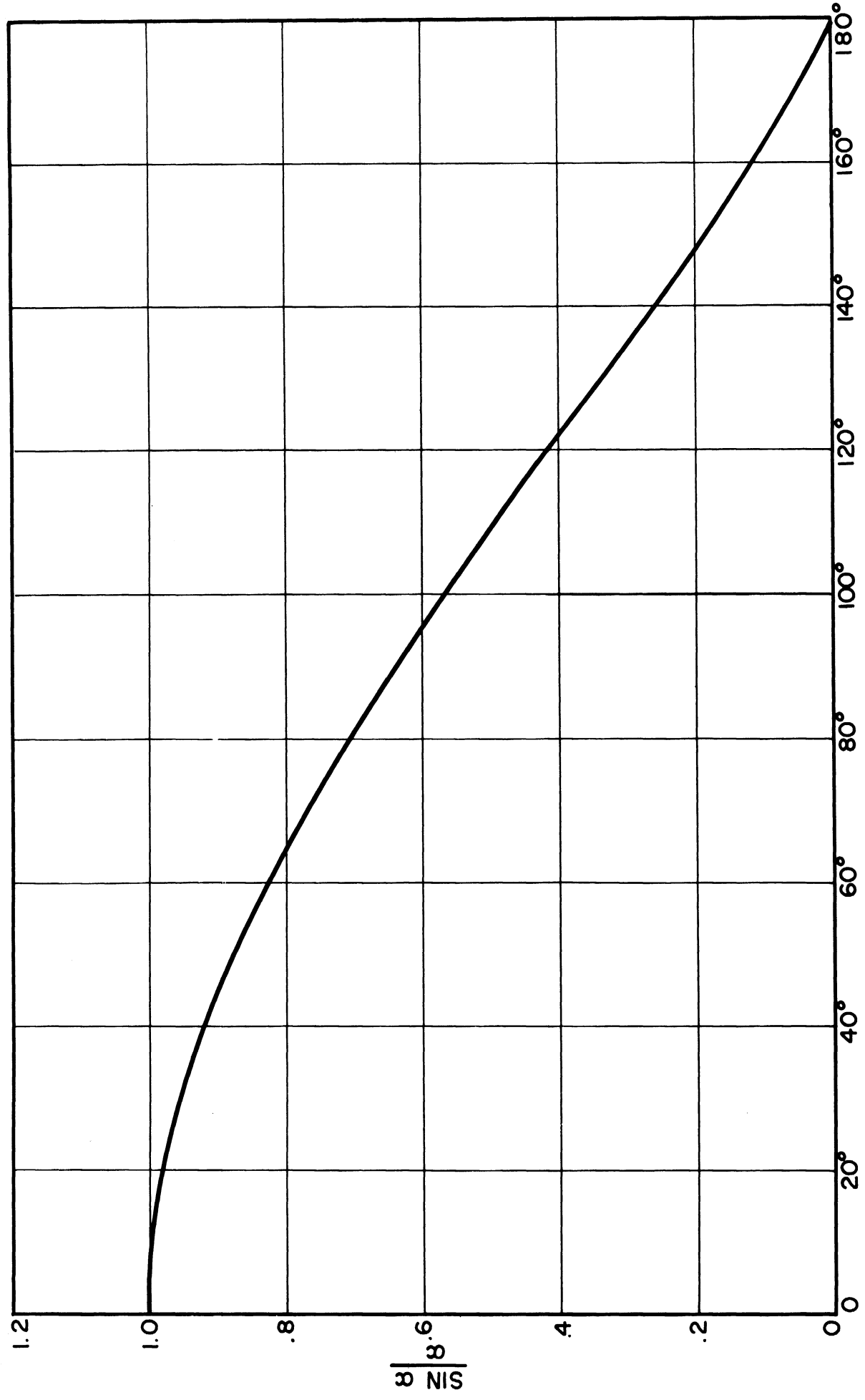

FIG. 2.3
FACTOR PRESENT IN EQUATIONS (2.20) & (2.23)

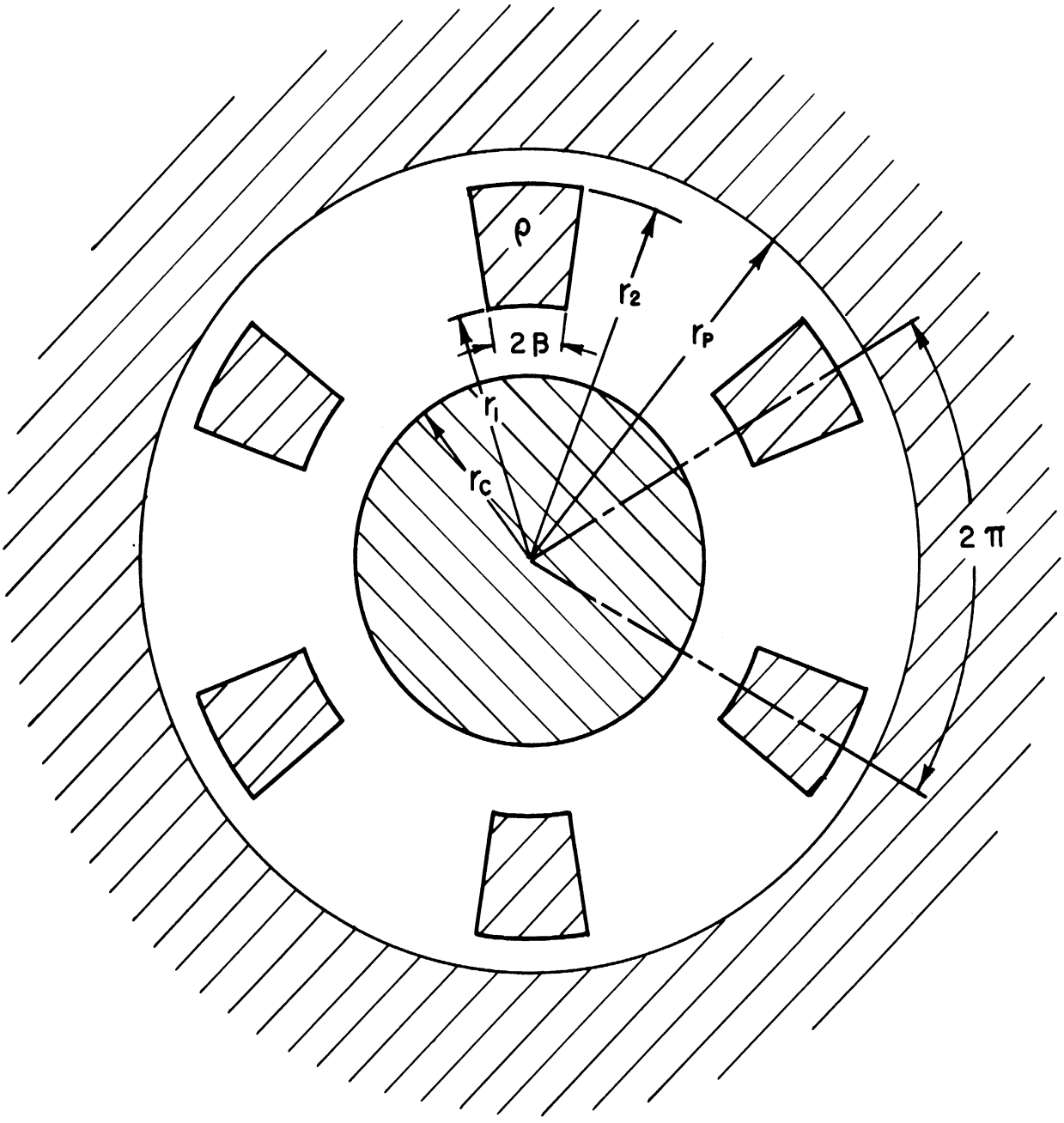

FIG. 2.4
SPACE CHARGE CONFIGURATION ASSUMED

r_2, r_1 and β are defined in Figure 2.4. Note that

$$\int_{r=r_1}^{r=r_2} \pi B_1 L \, r\,dr = \pi B_1 L\left(\frac{r_2^2 - r_1^2}{2}\right)$$

$$= \frac{\sin\beta}{\beta} \leq 1 \text{ as indicated previously.}$$

Now we are in a position to compute the function F using the A_1 and B_1 just derived

$$F = L\, r_c^2 \int\left(\frac{\pi A_1}{2}\right) \pi B_1 R\, d\,R \qquad 2.25$$

$$= 2\left(\frac{\sin\alpha}{\alpha}\right)\left(\frac{\sin\beta}{\beta}\right)\left(\frac{1}{R_a^{N/2} - R_a^{-N/2}}\right)\left(\frac{1}{R_2^2 - R_1^2}\right)\int_{R_1}^{R_2}\left(R^{N/2+1} - R^{1-N/2}\right) dR \qquad 2.26$$

where

$$R_1 = \frac{r_1}{r_c} \qquad \text{and} \qquad R_2 = \frac{r_2}{r_c} \ .$$

$$F = 2\left(\frac{\sin\alpha}{\alpha}\right)\left(\frac{\sin\beta}{\beta}\right)\left(\frac{1}{R_a^{N/2} - R_a^{-N/2}}\right)\left(\frac{1}{R_2^2 - R_1^2}\right)\left(\frac{R_2^{N/2+2}}{N/2+2} + \frac{R_2^{2-N/2}}{N/2-2} - \frac{R_1^{N/2+2}}{N/2+2} - \frac{R_1^{2-N/2}}{N/2-2}\right)$$

for $\left(\frac{N}{2} \neq 2\right)$. 2.27

For this case we see that F is determined by the tube geometry and the dimensions and location of the spoke.

One more point remains to be clarified before we proceed to a numerical example. Substituting equation 2.24 into 2.11 we note that

$$I_{km} = 4\,\beta L\,(r_2^2 - r_1^2)\,\rho\, f\, F \qquad 2.28$$

(F is defined above),

and for a solution the space-charge density must be given even though F is known. For the present we will use the relation

$$\rho = -2\epsilon_o \frac{m\omega_f}{e(N/2)} \left(\frac{N}{2}\omega_c - \omega_f\right)^5 \qquad 2.29$$

which was derived in an earlier report[6] from the Lorentz equation by assuming synchronous velocity, zero angular field, and constant radial motion for the charges.

---

5 Note that space-charge density, areas, etc., must be given in units corresponding to π units of angle between adjacent anode segments.

6 Technical Report No. 1, November 15, 1948

A Numerical Example

We will now apply these relations to the Model 3 magnetron which was used in the experiments recorded in the last Quarterly Report.

Given:

$r_a = 0.45$ cm

$r_c = 0.27$ cm

$R_a = 1.66$

$N/2 = 6$

$L = 0.66$cm

$f = 1{,}790$ mc

$B = 0.1950$ webers

$\alpha = 45°$

$\omega_c = eB/m = 3.43 \times 10^{10}$

$\omega_f = 2\pi f = 1.13 \times 10^{10}$

Assume:

$\beta = 45°$

$r_2 = r_a$

$r_1 = r_n$ = synchronous radius

$$= r_c \sqrt{\frac{N/2\ \omega_c}{N/2\ \omega_c - 2\omega_f}} \qquad = 1.06\ r_c$$

Then using equation 2.29

$$\rho = -0.0368 \text{ coulombs/m}^3.$$

Also,

$$\frac{\sin \alpha}{\alpha} = \frac{\sin \beta}{\beta} = 0.90,$$

$$\frac{1}{R_a^{N/2} - R_a^{-N/2}} = \frac{1}{21},$$

$$\frac{1}{R_2^2 - R_1^2} = \frac{1}{1.63}, \text{ and}$$

$$\frac{R_2^{N/2+2}}{N/2+2} + \frac{R_2^{2-N/2}}{N/2-2} - \frac{R_1^{N/2+2}}{N/2+2} - \frac{R_1^{2-N/2}}{N/2-2} = 6.69.$$

Therefore, using equation 2.27,

$$F = 0.316$$

and 2.28 gives

$I_{km} = -5.21$ amperes/anode pair, so that the induced current is

$\frac{N}{2} I_{km} = -31.2$ amperes.

This number seems to be high, especially so if a comparison is made between this figure and the r-f current calculated for this tube in Section 3 of the last Quarterly report.[7] There, the r-f current was determined by using an equivalent circuit in conjunction with experimental information, and the result must be judged as fairly accurate. R-m-s values of the order of .1 ampere were obtained. This conclusion indicates that our answer is in error by a factor of 20 or 30.

Such a serious discrepancy does not invalidate our induced current technique. However, it does seem to indicate that the choice of

---

7 Quarterly Progress Report No. 2, July, 1950. See particularly Figure 3.8.

spokes assumed was seriously in error. One way to correct this difficulty would be merely to assume that the space-charge density of the spoke was less than that chosen in this example. One could readily obtain a desired answer by this method since the induced current and the space-charge density of the spoke are proportional. Evidently we would be forced to abandon the space-charge density formula given in equation 2.29 if this procedure were followed.

An alternative is as follows. Suppose we imagine the interaction space to be made up of a synchronously moving constant space-charge density cloud satisfying equation 2.29 plus a small superimposed distribution of spokes with space-charge density ρ_{spoke}. The constant part of the space-charge cloud makes no contribution to the induced current, but by slowly drifting toward the anode accounts for the direct current. Under such circumstances the superimposed spokes account for most of the r-f current by induction, and only small contributions are made to the r-f and the d-c by the arrival of charges from the spokes to the anode.

Suppose we accept this picture briefly and assume the superimposed spokes have the form of the last example. In addition assume that the maximum value of the r-f induced current is one ampere and that the d-c current is one-half of this value.[8] Then the d-c part of the synchronous space charge has the value computed previously, and the superposed spoke density is

$$\frac{100\,\rho_{spoke}}{\rho_0} = \frac{100}{31.2} = 3.2\ \%\ \text{of this value.}$$

---

[8] Loc. cit. for a justification of such a choice of currents.

We now have an approximate method for checking this answer since it is related to the currents and transit-time. Considering that our whole synchronous cloud is drifting toward the anode with a velocity v_r. Then the d-c current is approximately given by

$$2\pi \frac{N}{2} r_a L v_r \rho$$

Equating this to one-half of the induced current gives

$$2\pi \frac{N}{2} r_a L v_r \rho \simeq 2 \frac{N}{2} \beta L (r_2^2 - r_1^2) \rho_{spoke} f F \qquad 2.30$$

by equation 2.28. Substituting in the known values,

$$v_r \cong 6.05 \times 10^5 \text{ cm/sec.}$$

We also know the angular velocity of the charge

$$\omega_n = \frac{\omega_f}{N/2} \qquad 2.31$$

so that we can easily estimate the number of revolutions a charge makes during its transit time across the interaction space. This is the check desired. For the present case about 80 revolutions are undertaken by charges making their transition across the Hartree space.

This number of revolutions seems excessively high. An alternative proposal made previously was to abandon the space-charge density relation 2.29, assume the well defined spokes shown in Figure 2.4 without the d-c base, and adjust the density of the spoke to give the experimentally observed current. We will see that under these circumstances the transit time across the interaction space is considerably reduced. Suppose now that we accept this picture and proceed as before. In addition we assume that the r-f component of the induced current is one ampere and that the

d-c current is one-half of this value just as we did in the last case.

This gives

$$\rho = \frac{-0.0368}{31.2} = -0.00118 \text{ coulombs/m}^3.$$

For the assumed space-charge configuration the d-c current is

$$2\pi \frac{N}{2} r_a L v_r \rho \frac{\beta}{\pi} \qquad 2.32$$

Equating this to one-half of the r-f component of the induced current

$$2\pi \frac{N}{2} r_a L v_r \rho \frac{\beta}{\pi} = 2 \frac{N}{2} \beta L(r_2^2 - r_1^2) \rho f F, \qquad 2.33$$

and a substitution of values gives

$$v_r = (125)\ (6.05 \times 10^5) \text{ cm/sec}$$

This answer is (125) times the radial velocity obtained in the last case so that we may expect charges to execute about $\frac{80}{125} \simeq 2/3$ of a revolution in crossing the Hartree space. This answer is more nearly what might be anticipated. The transit time corresponds to about seven Larmor periods.

We refrain from conclusions at this early stage in our induced current studies except to point out that they reflect serious doubt on the tenability of the space-charge density equation 2.29.

3. TRANSIT TIME AND MAXIMUM CURRENT BOUNDARY (S. Ruthberg, H.W. Welch, Jr.)

This section contains some calculations based on the static magnetron solution which place limitations on the amount of current which can be drawn in an oscillating magnetron. The possibility is indicated that transit time may have some correlation with the maximum current boundary.

If the striated-type solution discussed by Slater is assumed for the swarm,[1] then the maximum current is found in the single-striated case, where the electrons reach the swarm boundary in one quasi-cycloidal arc. If further, it is assumed that the plane magnetron solution is similar to the cylindrical case, then the transit time for a particle through the swarm is just the cyclotron period

$$T_c = \frac{2\pi}{\omega_c} = \frac{\pi}{\omega_L} \qquad 3.1$$

where ω_c and ω_L are the cyclotron and Larmor angular velocities respectively. This is the minimum time in which charge can be transported across a striated region, and hence, in this case to the boundary.

The type of discharge is then dictated by the amount of charge transported through the spokes to the anode posts. This can be found by knowing the d-c anode current and the time during which it is delivered. This time can be estimated as follows: If the number of wave lengths of r-f in the circumference of the magnetron is one-half the number of anode

---

[1] J. C. Slater, Microwave Electronics, D. Van Nostrand, 1950, New York, Chap. 13.

posts, the r-f wave advances the distance of two geometric sectors in one r-f period. Consider a well defined spoke having the same width as the anode post as was done in the last section. As the spokes rotate at the synchronous angular velocity, an anode post draws current for one-half an r-f cycle. This gives the synchronous angular velocity as

$$\omega_n = \frac{2\pi f}{n}$$

where f is the r-f frequency and n is the number of wave lengths λ, in the circumference.

A method for estimating the maximum space charge limited current (I_{An}) for the oscillating magnetron was given in Section 5 of the last Quarterly Progress Report with the following result.

$$I_{An} = \alpha_n \left(\frac{I_{Ln}}{I_{Lo}} \right) I_{Lo} \qquad 3.2$$

α_n = a function of r_n/r_c defined by Slater and given in Figure 5.1 of the last Quarterly Report

$\frac{I_{Ln}}{I_{Lo}}$ = ratio of Langmuir current at the synchronous radius to the Langmuir current at the anode with E_n assumed at synchronous radius and E_o assumed at the anode radius.

$E_n = \frac{1}{2} \frac{m}{e} \omega_n^2 r_a^2$

$E_o = \frac{1}{2} \frac{m}{e} \omega_n^2 r_a^2$

r_n = synchronous radius

r_a = anode radius

I_{Ln}/I_{Lo} is also a function of ratio of anode to cathode radius and of magnetic field. It is given in Figure 5.2 of the last Quarterly Report.

Using the value of the current given by equation 3.2 with the period of one-half the r-f cycle, we can calculate the charge which must be delivered to the anode each cycle.

$$q = -\alpha_n \left(\frac{I_{Ln}}{I_{Lo}}\right) \frac{I_{Lo}}{2f} \qquad 3.3$$

By definition

$$I_{Lo} = \frac{8\pi}{9} \varepsilon_o \sqrt{\frac{2e}{m}} \frac{L}{r_a} \frac{E_o^{3/2}}{\beta_a^2}$$

which is the Langmuir relationship. Also

$$f = \frac{n\omega_n}{2\pi}$$

Using the definition of E_o therefore

$$q = -\frac{4\pi^2}{9} \varepsilon_o \frac{\alpha_n}{n} \left(\frac{I_{Ln}}{I_{Lo}}\right) \frac{m}{e} \frac{\omega_n^2 r_a^2}{\beta_a^2} L \qquad 3.4$$

The total charge in the hub of the space charge swarm is given by

$$\tau = -2\pi\varepsilon_o \frac{m}{e} \omega_L^2 r_n^2 \left(1 - \frac{r_c^4}{r_n^4}\right) L \qquad 3.5$$

L = length of cathode

This can be shown to be true no matter what distribution exists within the swarm so long as there is no radial velocity at the boundary. The factor r_n may be eliminated from this equation by using the angular velocity relationship which is

$$\left(\frac{r_n}{r_c}\right)^2 = \frac{\omega_L}{\omega_L - \omega_n} \qquad 3.6$$

By making this substitution, equation 3.5 may be written as follows:

$$\tau = -2\pi \varepsilon_o \frac{m}{e} \omega_n \omega_L \frac{2\omega_L - \omega_n}{\omega_L - \omega_n} L \qquad 3.7$$

Thus, with equation 3.4, we are able to calculate the ratio of the charge delivered per cycle to the charge existing in the swarm under static conditions.

$$\frac{q}{\tau} = 2\pi \frac{\alpha_n}{n\beta_a^2} \frac{I_{Ln}}{I_{Lo}} \frac{\omega_n}{\omega_L} \frac{\omega_L - \omega_n}{2\omega_L - \omega_n} \frac{r_a^2}{r_c^2} \qquad 3.8$$

In order to obtain some idea of the orders of magnitude involved this is applied to the Model No. 3 magnetron which was discussed in Section 3 of the last Quarterly Progress Report. Further data were given on this tube in Technical Reports No. 1 and No. 2.

We have:

$r_a = .45$ cm

$r_c = .27$ cm

$B = 1950$ gauss (not given with data in last Quarterly Report)

$B_o = 329$ gauss $\left(= 2\frac{m}{e} \cdot \omega_n \frac{1}{1-(r_c^2/r_a^2)}\right)$

$B/B_o = 5.9$

$L = .66$ cm

$e/m = 1.76 \times 10^{11}$ coulombs/Kgm

$\varepsilon_o = \frac{1}{36\pi} \cdot 10^{-9}$ farad/meter

$n = 6$

$E_o = 196$ volts.

Thus

$\omega_L = 1.75 \times 10^{10}$ rad/sec,

$\omega_n = 1.85 \times 10^{9}$ radians/sec.

From equation 3.6

$$r_n/r_c = 1.06,$$

and from Figure 5.1 in Quarterly Progress Report No. 2

$$\alpha_n = .72 .$$

From Figure 5.2

$$I_{Ln} / I_{Lo} = 22$$

Langmuir's constant for $r_a/r_c = 1.66$

$$\beta_a^2 = .18. \quad (2)$$

Using these figures the transit time through the hub is found to be 1.8×10^{-10} sec; the time of current flow to an anode post per cycle is 2.82×10^{-10} sec. (1/2 cycle). The transit time through the swarm is, therefore, of the same order as the time of current flow.

Using equation 3.8 we find the ratio q/τ to be 1.45. That is, if the tube were to have a space charge limited maximum current boundary then, for the case discussed, the charge drawn over per r-f cycle is considerably greater than the total contained in the swarm under static conditions.

It is of interest to compare this result with the value obtained when the 1/2 Allis current is used for the maximum current boundary (as suggested by Slater). In the notation used here the 1/2 Allis current is given by

$$\frac{1}{2} I_{Aa} = \frac{\alpha_a}{2} \left(\frac{B}{B_o}\right)^3 I_{Lo} \qquad 3.9$$

This value of current is about five times greater than the value I_{An} used in the above calculation. In either case the space charge swarm can not be considered a reservoir of charge. It should be pointed out that one reason the 1/2 Allis current is so much larger is that it is

---

[2] W. G. Dow, "Engineering Electronics", p. 535, Wiley, New York, 1937.

assumed that the voltage on the anode has reached the cutoff value which, in this case, is three times greater than the starting voltage.

We may conclude that the swarm is definitely depleted during a cycle if the current assumed in these calculations is drawn. Since there are only about three transit-time periods to 1 r-f cycle the question arises as to how quickly the swarm configuration can be reestablished. If it should require several transit-time periods, then the maximum current boundary might be expected to occur at a much smaller current than the one assumed above. Also, since the swarm does not act as a reservoir, the emission current from the cathode must definitely be considered. Upon examination of the experimental results on the Model 3 given in the last Quarterly Report (Figure 3.8, page 24) we find an observed current maximum of .37 ampere. The value given by equation 3.2 is 5.3 amperes, a factor of approximately 15 greater. The value obtained by removing all the charge in one-half the r-f cycle is 3.6 amperes, or almost ten times greater. It would appear that the current limitation in the actual case is not explained on the basis of space charge limitation making the effects due to transit time plausible.

A rough estimate of the minimum value of transit time through the spokes may be made by considering current through rectangular spokes as a parallel electrode case following the Child-Langmuir distribution. In this case the transit time is given by

$$T = k \frac{d_{ca}}{v_a} \qquad 3.10$$

where k is 2 when no space charge exists and 3 when space charge exists. d_{ca} is the distance between the two "electrodes" and v_a, the velocity of the particles at the anode.

If we assume one end of the spoke at the synchronous potential of the swarm hub edge, E_n, and the other at the Hartree potential, E_h, then,

$$1/2\ m\ v_a^{\,2} = e\ (E_h - E_n)$$

and

$$v_a = \sqrt{\frac{2e}{m}}\ (E_h - E_n)^{1/2}$$

Using 3.10

$$T = k \sqrt{\frac{m/2e}{(E_h - E_n)}}^{1/2}\ d_{ca} \qquad 3.11$$

For the case discussed

$$E_n = 102 \text{ volts}$$

$$E_h = (2\,\frac{B}{B_o} - 1)\ E_o = 2100 \text{ volts}$$

We will assume that $d_{ca} = r_a - r_n = .43$ cm

and that $k = 3$. Then

$$T = 3\sqrt{m/2e}\ \frac{.43 \times 10^{-2}}{(1998)^{1/2}}$$

$$= 4.9 \times 10^{-10} \text{ seconds,}$$

or of the order of 90 per cent of the r-f cycle. The time must actually be much greater than this because of the confining effect of the magnetic field.

The calculations given above should not be taken seriously except as they represent upper and lower limits on the quantities involved. More rigorous methods will be attempted but the complexity of the problem does not offer much encouragement for results in the near future. Our main hope for practical analysis lies in the possible discovery of some method for simplification of the problem which does not require excessive distortion of the physical picture.

4. EXPERIMENTAL STUDY OF MAGNETRON PERFORMANCE (H. W. Welch, Jr.)

In the last Quarterly Report experimental results on a Model 3 magnetron were presented in connection with the discussion of frequency pushing. There was also presented a discussion of low Q operation and the factors involved, particularly maximum current boundary, magnitude of pushing, effects of cathode temperature and loading condition. The problem resolves itself to a more complete analysis of effects of all variables in magnetron operation on formation and action of the space charge swarm. The number of variables and the small amount of available complete data make correlation of theory with experiment extremely difficult. It has been emphasized previously in these reports that many of the effects of space charge in conventional magnetrons can only be observed by taking measurements with an accuracy of between one-tenth and one per cent.

The experiments reported on in the present section are incomplete. Some interpretation is given but complete analysis will be reserved until the theory has been developed further and more experimental information is available.

The magnetron used in these experiments was Model 7A, No. 33. An assembly drawing is given in Figure 4.1. This tube was built to be used in experimental work in the study of maximum current boundary. Two outputs were provided, one coupled to the desired 14-cm mode and one to the undesired 9-cm mode. Thus by selective loading of the two loops it was hoped that mode separation could be changed and the effect on maximum current boundary observed. Actually the effect of loading does not seem

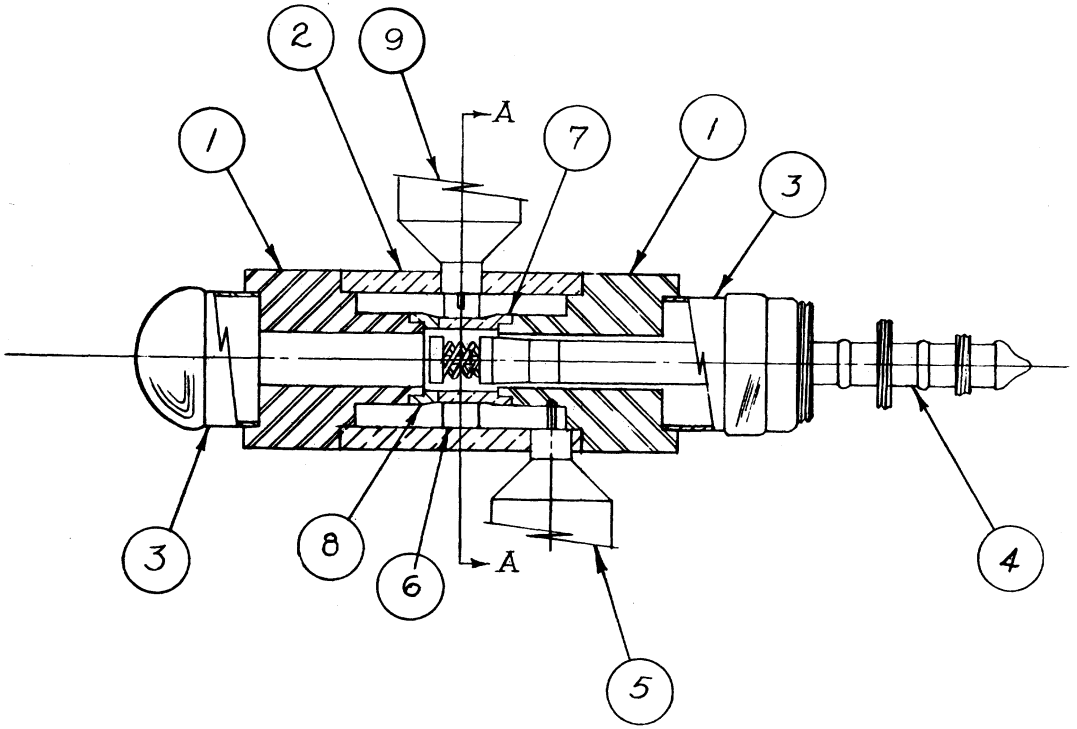

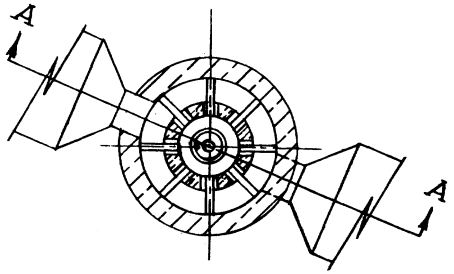

SECTION A-A

FIG. 4.1

ALL DIMENSIONS UNLESS OTHERWISE SPECIFIED MUST BE HELD TO A TOLERANCE - FRACTIONAL ± 1/64" DECIMAL ± .005" ANGULAR ± 1/2°

		ENGINEERING RESEARCH INSTITUTE UNIVERSITY OF MICHIGAN ANN ARBOR MICHIGAN	DESIGNED BY HWW	APPROVED BY
			DRAWN BY	SCALE FULL
			CHECKED BY RES	DATE
		PROJECT M-762	TITLE CO-AXIAL MAGNETRON MODEL 7A	
1	7-20-50	CLASSIFICATION	DWG. NO. B- 10,007A	
ISSUE	DATE			

to be sufficient to bring the two modes into competition. Mode separation is quite adequate, more than 30 per cent. The tube jumps completely out of oscillation in one mode before any oscillation is observed in the other.

Some of the test results are recorded in Figures 4.2 to 4.7. The results given show the effect of magnetic field and cathode temperature on tube performance. This tube is particularly interesting in that a very pronounced effect of the space charge on operation is observed near the cyclotron resonance.[1] This is shown in the performance characteristics of Figure 4.2. The maximum current boundary goes through a fairly sharp minimum and the oscillatory wave length makes a sharp jump at the cyclotron field. The cyclotron field is calculated from the simple relationship

$$\frac{2\pi c}{\lambda} = \frac{Be}{m} \qquad 4.1$$

The effects are made more obvious by the graph of Figure 4.3. The wave length for which oscillation starts and the maximum current for oscillation are plotted against magnetic field.

No interpretation of the effect on maximum current boundary will be offered at this writing. One may speculate that some sort of zero order mode may exist similar to that observed in rising sun tubes or that perturbation of the electron stream near the cyclotron resonance upsets conditions of synchronism. Neither answer can be substantiated without further study. The effect is quite obviously due to space charge, as study of the resonant wave length can show. The resonant wave length of the tube with cathode hot is indicated on Figure 4.3 and Figure 4.6.

---

[1] This effect was also observed on another magnetron with the same interaction space design but different resonant circuit. See the discussion of Model 4 of Section 2 of the interim report of December 15, 1949.

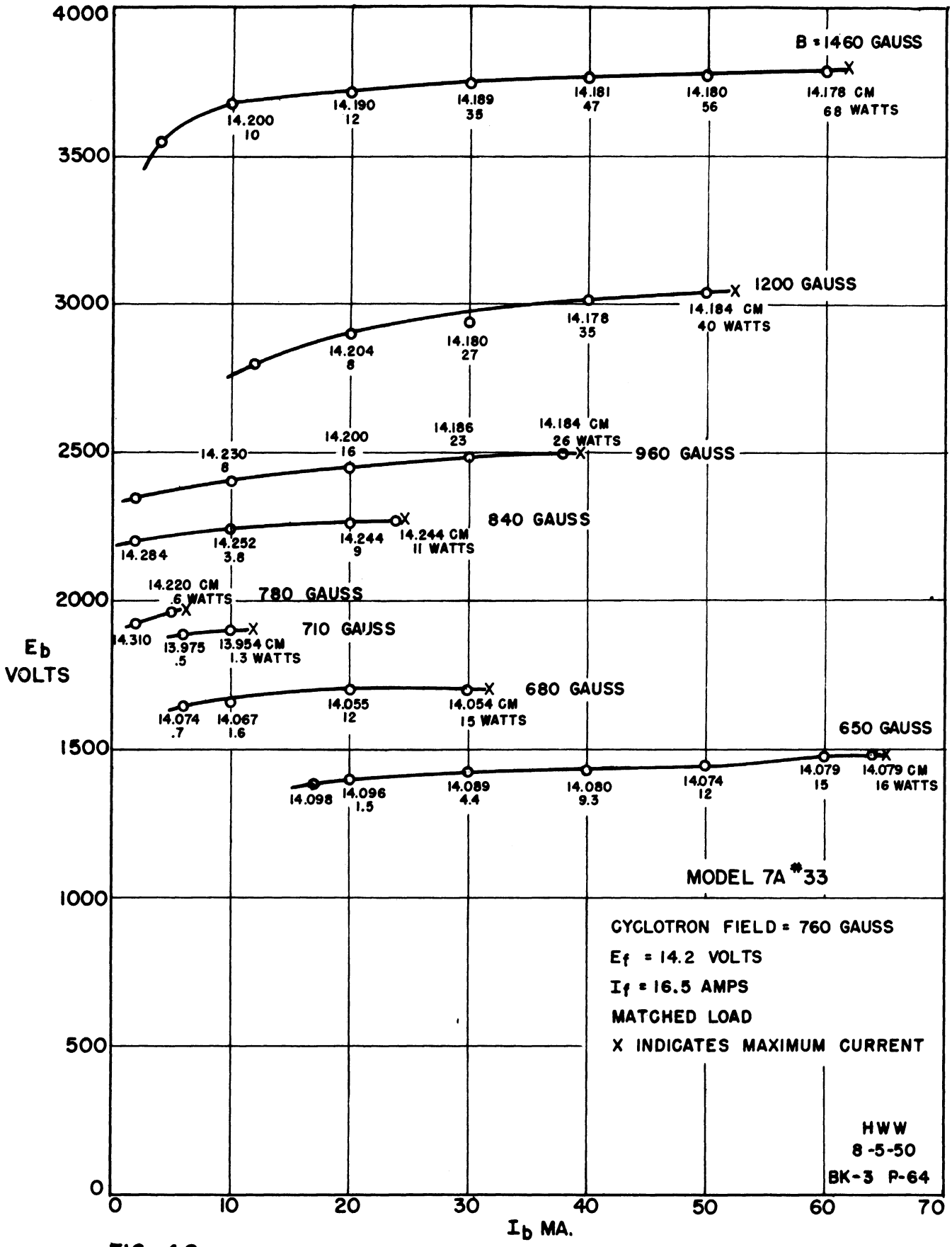

FIG. 4.2

PERFORMANCE CHARACTERISTICS MODEL 7A #33. SHOWING EFFECT OF CYCLOTRON RESONANCE ON MAXIMUM CURRENT BOUNDARY AND WAVELENGTH.

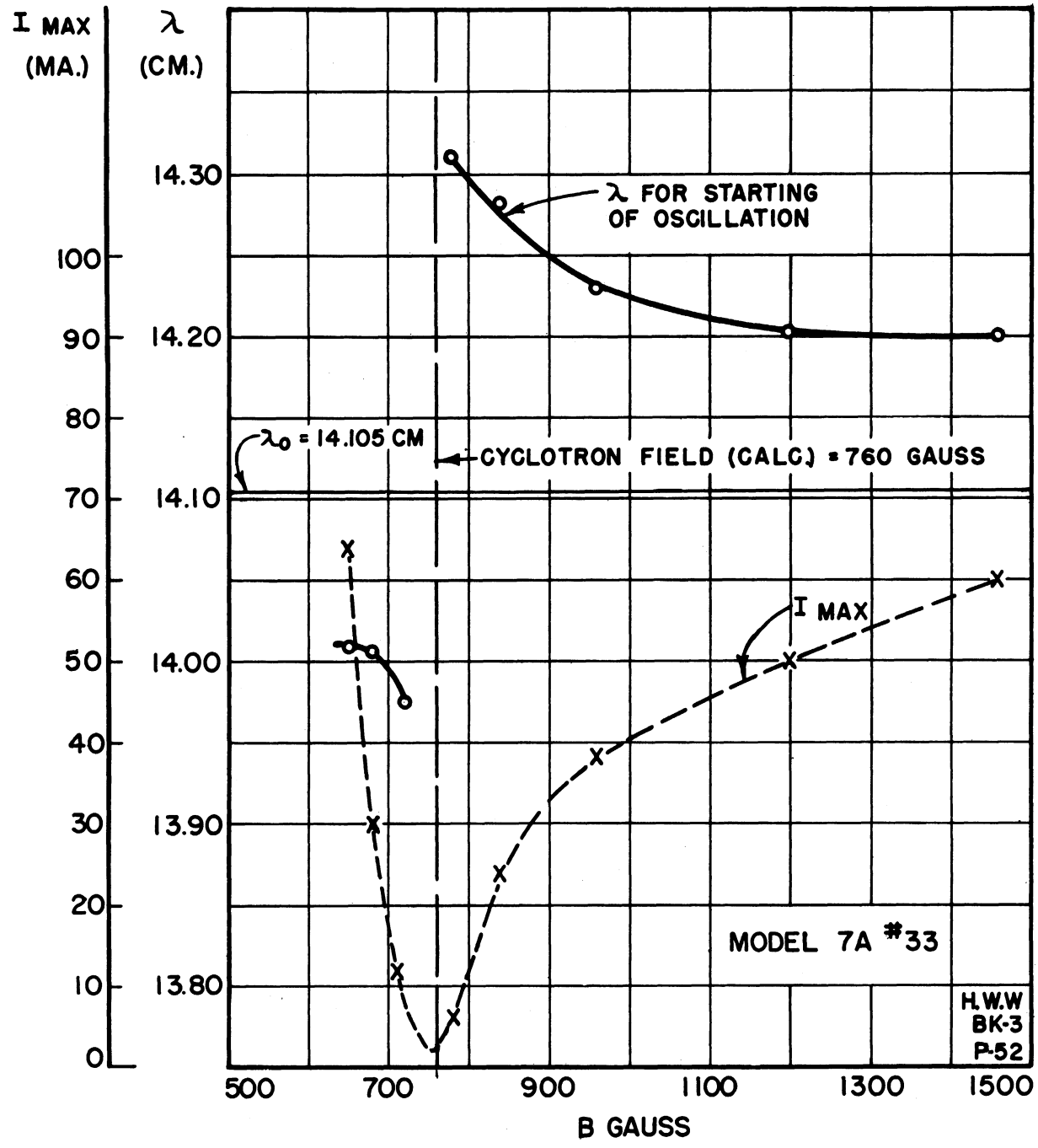

FIG. 4.3

MAXIMUM CURRENT BOUNDARY AND STARTING WAVE-LENGTH AS A FUNCTION OF MAGNETIC FIELD

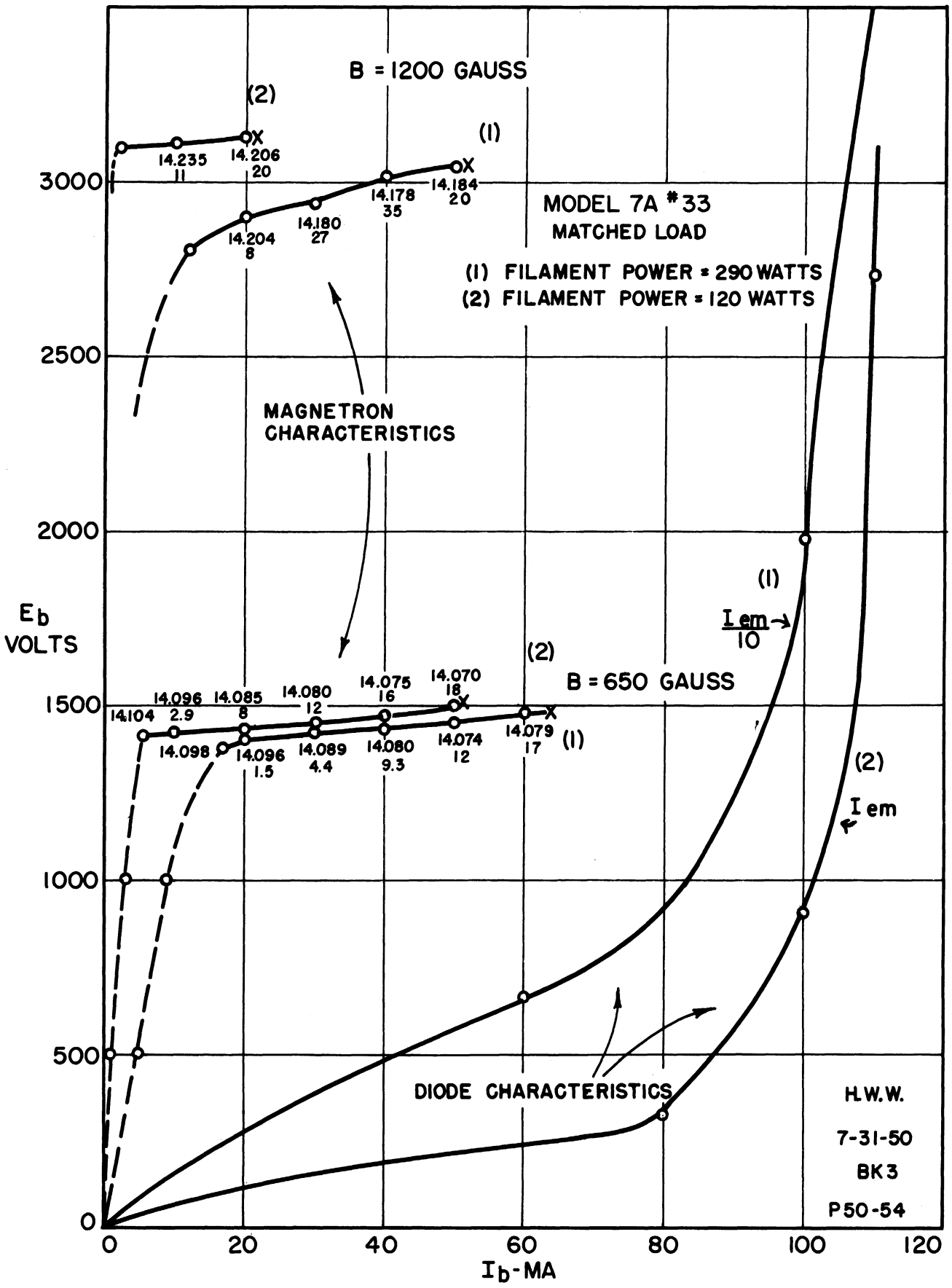

FIG. 4.4
COMPARISON OF MAGNETRON CHARACTERISTICS WITH DIODE CHARACTERISTICS.

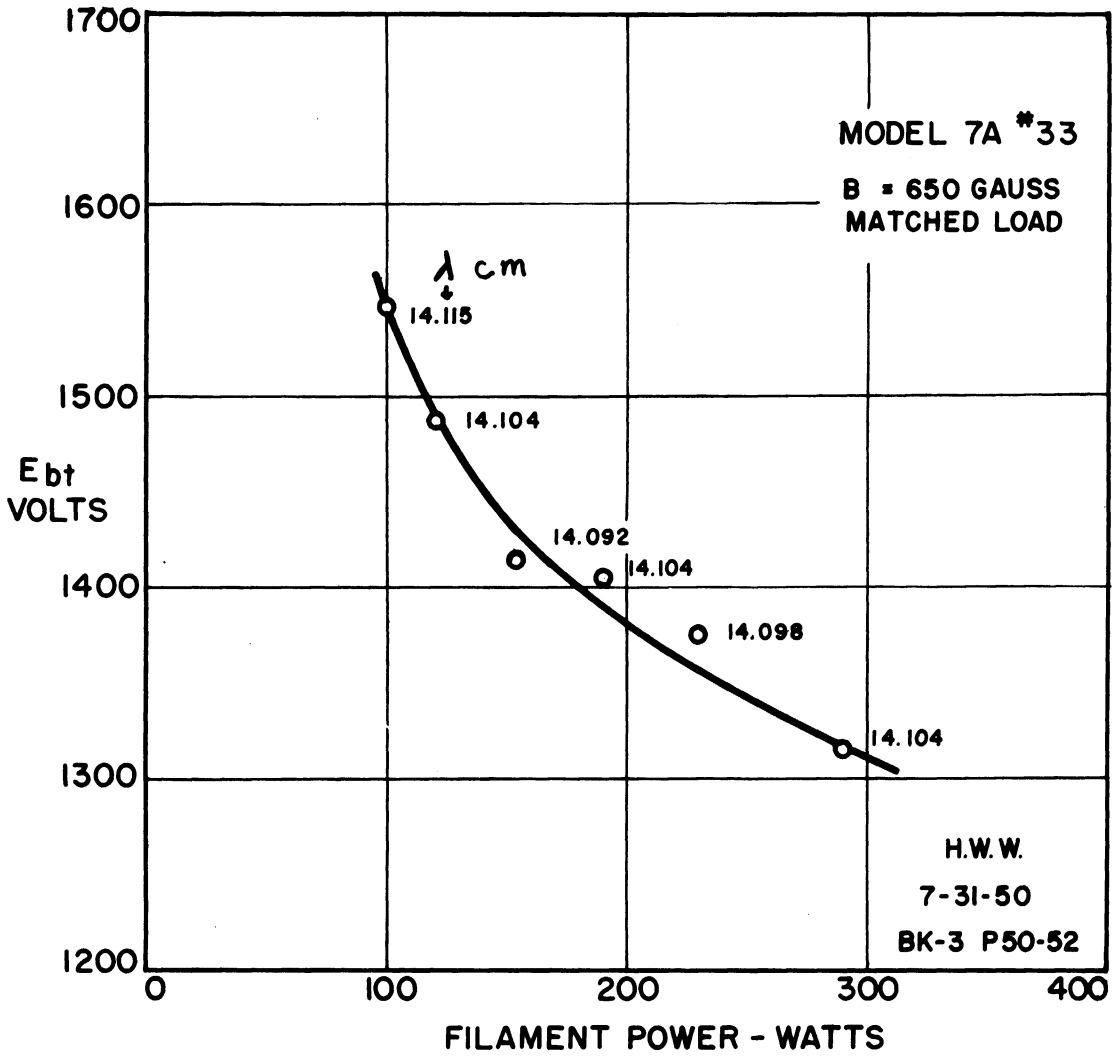

FIG. 4.5
OBSERVED STARTING VOLTAGE AS A FUNCTION OF FILAMENT POWER

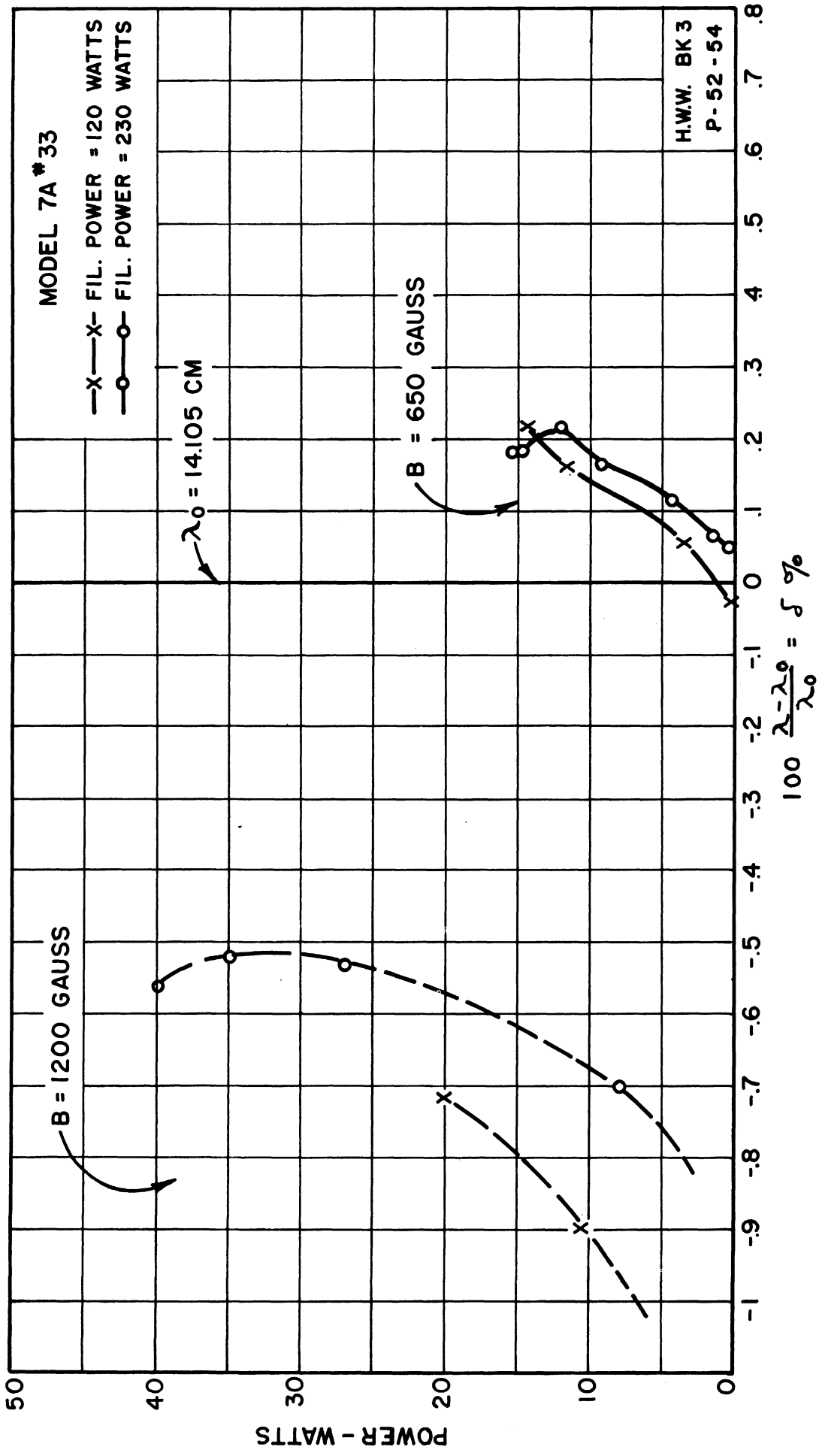

FIG. 4.6
EFFECT OF MAGNETIC FIELD AND EMISSION ON PUSHING CURVES

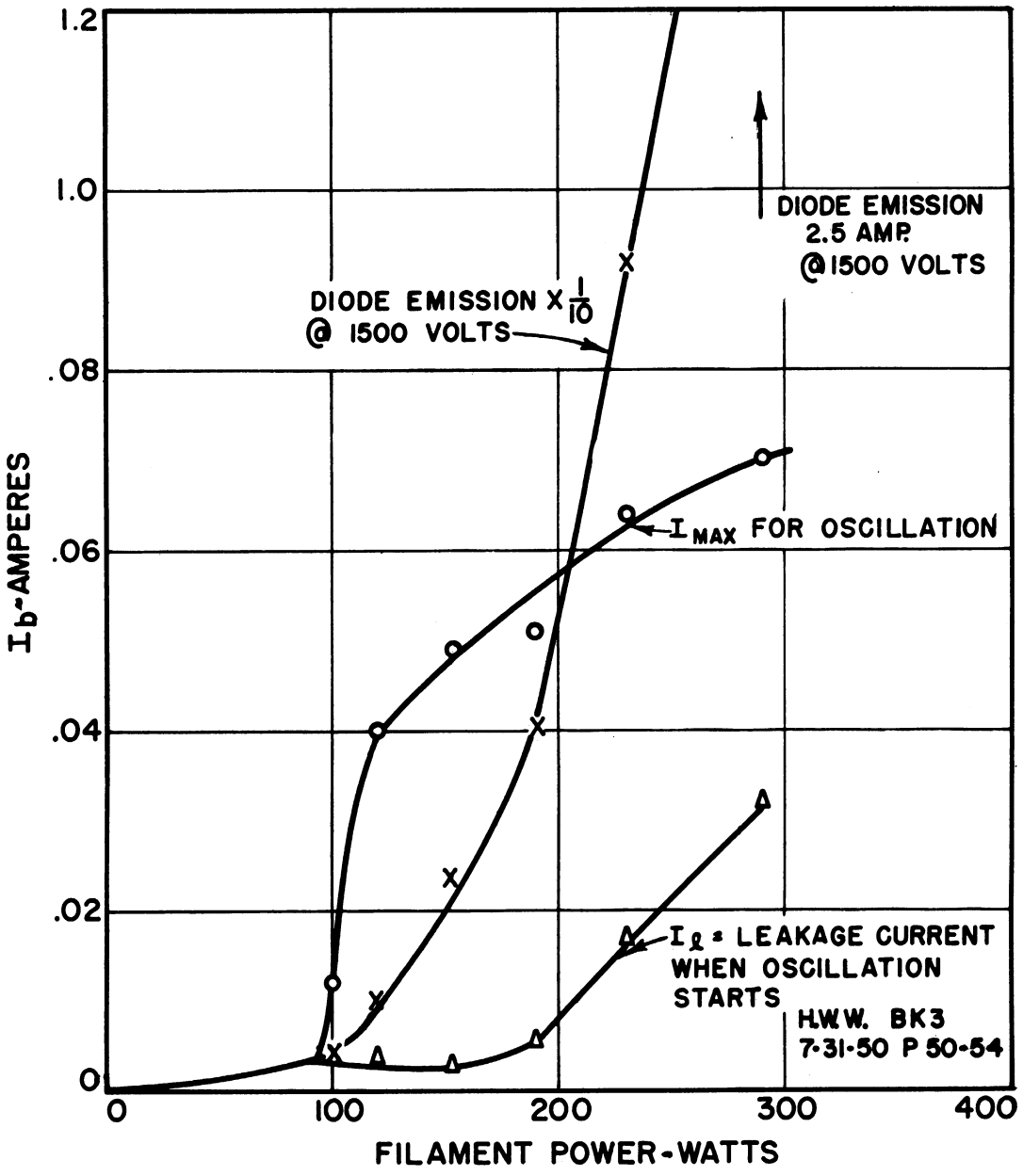

FIG. 4.7
COMPARISON OF MAXIMUM CURRENT BOUNDARY, LEAKAGE CURRENT AND DIODE EMISSION MODEL 7A #33

For fields lower than the cyclotron field the oscillations start at a shorter wave length than the resonant wave length. This is very unusual in magnetrons. At the higher fields the customary behavior is observed. Oscillation starts at a longer wave length than the resonant wave length. This type of behavior has been discussed in some detail in previous reports.[2]

The measurement of resonant wave length as a function of anode voltage by hot impedance tests shows that for magnetic fields well above the cyclotron field the resonant wave length is increased by expansion of the space charge swarm, and, for fields less than the cyclotron field the resonant wave length is decreased by this expansion. This result is also predicted by the theory. (See Quarterly Report No. 1.) Measurements of resonant wave length of the Model 7A at voltages insufficient to support oscillation show the expected behavior, thus offering an explanation for the frequency shift at the cyclotron field. These measurements are summarized in Table 4.1 below.

Table 4.1

Results of Hot Impedance Measurements on Model 7A No. 33

B = 650 gauss E_f = 14.2 volts I_f = 16.5 amps.

E_b volts	I_b amp.	λ_o cm	Q_1	Q_o	Q_{ext}
0	0	14.105	113	236	151
500	.007	14.072	83	187	154
1000	.012	14.105	164	740	174
1400	.011	14.098	Oscillation observed.		

[2] See pages 7 to 13 of the Quarterly Report No. 2, also Quarterly Report No. 1 and Technical Report No. 1.

Note that the wave length has decreased for the 500-volt measurement and is back to the original value for the 1000-volt measurement. This reversal of the direction of wave length shift is attributed to synchronous effects in the space charge and has been shown in other data given in the first Quarterly Report. The effect of synchronism also shows up in the unloaded $Q(Q_o)$ which increases from 187 to 740 as the anode potential is raised from 500 volts to 1000 volts. More measurements of this type will be taken at other magnetic fields.

The effects of cathode temperature are shown in Figures 4.4 to 4.7. In Figure 4.4 volt-ampere characteristics at two different magnetic fields and two different cathode temperatures are given. For comparison, diode characteristics (no magnetic field) are given on the same chart. (Note that the scale of one of the emission curves has been divided by 10 so that available emission is actually approximately 10 times greater for the curves numbered (1) than it is for curves numbered (2). It is evident that the maximum current boundary is not proportional to the available emission in this case. This is more obvious in Figure 4.7 where the leakage current (current for which oscillation is first observed), the maximum current boundary and the diode emission are plotted for comparison. Above 150 watts cathode power the difference between leakage current and the maximum current boundary remains substantially constant, while in the same range the diode emission varies by a factor of 10. The leakage current in this tube is probably due to end hat emission; therefore, one would conclude that the current in interaction space is unaffected by emission in this case. However, as the cathode power is reduced from about 150 watts to 100 watts the maximum current boundary is definitely reduced and appears to go to zero at about 90 watts.

The effect of cathode temperature on starting voltage is very definite. Figure 4.5 shows data taken from a number of characteristics like those in Figure 4.4. Starting wave length does not appear to be affected strongly although the data in Figure 4.6 indicate otherwise. The effect on starting voltage may be useful in interpreting space-charge behavior. For example it may be related to the initial velocity distribution for the electrons. Theoretical analysis has not yet produced any satisfactory explanation.

Data of the type shown in Figure 4.6 show no very startling effects of emission on pushing curves. The data are not yet complete, however, and one should be careful in drawing too many conclusions.

Measurement of the effect of load on performance has been started and so far has indicated that in this particular tube, the load has a relatively small effect on maximum current boundary. This fact and the fact that cathode temperature has very little effect on maximum current boundary over quite a wide range make the behavior of this tube especially interesting because it does have a low maximum current boundary. The effect of mode competition has also been eliminated and the current does not approach space charge limited value given in Section 5 of the last Quarterly Report. We are left with the causes we know least about, and which must be intimately related to details of the interaction space design.[3] Another tube is being built with the same geometry as Model 7A, No. 33 except for cathode. The cathode will be made larger to decrease the ratio of anode-to-cathode radius from 1.75 to 1.50. The results on this tube when available should help to increase our understanding of the effect of interaction space design on maximum current boundary.

---

3. See Quarterly Report No. 2, pages 26, 27.

5. R.F. PROPERTIES OF A MAGNETRON SPACE CHARGE -- (G. R. Brewer)

A. Theoretical Analysis

a. Review: In the previous quarterly report (July 1950) the results of a theoretical analysis of the propagation of electromagnetic waves in a magnetron-type space charge cloud was presented. This analysis was carried out under the following conditions or assumptions:

(a) The space charge cloud is considered as defined, as far as velocity and charge density are concerned, by the well-known Hull-Brillouin relations (although the results can be expressed quite generally so that any desired charge distribution can be used).

(b) The space charge cloud is considered as an ideal isothermal gas to which non-relativistic equations are applicable.

(c) The waves are considered as having certain prescribed field components and are interacting with the space charge in such a manner that the boundary effects can be neglected. That is, the space charge may be considered as of very small or very great extent as the case may be.

b. Collisional Loss in the Space Charge: It is well-known from experiment that the electrons in a magnetron space charge do not always pursue the regular ordered orbits as prescribed by the equations of motion, but that some of their ordered energy is converted, by some means not yet fully understood, into disordered or random energy. The phenomenon is probably related to the current drawn from a space charge under cut-off conditions and in fact the random energy has been measured by Linder[1].

---

[1] Linder, E. G., "Excess Energy Electrons and Electron Motion in High Vacuum Tubes," Proc. I.R.E., Vol. 26, p. 346, 1938.
Linder, E. G., "Effect of the High Energy Electron Random Motion on the Shape of the Magnetron Cut-Off Curve," J. App. Phys., Vol. 9, p. 331, 1938.

In case the motion is wholly or partially double stream or in case of any deflection from the regular path in the single stream cone, the electrons can strike the cathode, thus losing some of their energy.

The electrons, in their ordered motion, can strike neutral gas atoms and, while the probability of an exciting collision will be low, the ordered energy will in any event be converted partially into random energy.

By the above means (and probably others), an electron set in motion by an electric field can lose some or all of its energy. When this occurs a wave propagating through the medium will decrease in amplitude with distance, thus being attenuated. The inclusion of terms in the equations of motion to account for the loss by the first of the above mechanisms is difficult. However, Appleton and Chapman[2] have shown that the effect of electron-atom or electron-ion collisions in a plasma in the absence of magnetic field can be represented by a frictional-type force proportional to the velocity of the electron, i.e., as gv, where g is the inverse average time between collisions. Assuming this same type of frictional force to be present when a magnetic field is applied, the equation of motion of the electrons becomes

$$\frac{\delta \vec{v}}{\delta t} + g\vec{v} + (\vec{v}\cdot\Delta)\vec{v} = -\frac{e}{m}\left[\vec{E} + \vec{v} \times \vec{B}_o\right] \qquad 5.1$$

Using this equation instead of equation 9.1 of the previous quarterly report, relations may be derived for the complex index of refraction of the medium in an identical manner to that outlined in the last report. The

---

[2] Appleton and Chapman, "The Collisional Friction Experienced by Vibrating Electrons in Ionized Air", Proc. Phys. Soc. London, Vol. 44, p. 246, 1932.

results obtained when the loss term is included are tabulated below. It is seen that the real part of the index of refraction is the same as presented previously, since terms involving g^2 have been neglected in comparison with ω^2 or ω_c^2, a thoroughly justifiable approximation for all reasonable gas pressures in the magnetron (i.e., less than 10^{-6} mm Hg). Extrapolations from the data of Appleton and Chapman, and calculation of the mean time between collisions for assumed electron orbits, afford two methods of finding the numerical value of g for a given gas pressure; this value usually is of the order of $g = 0.5 \times 10^{-6}\omega$.

(a) Propagation in the direction of the magnetic field:

Plane magnetron:

$$\varepsilon_{eff} = 1 - \frac{1}{\left(\frac{\omega}{\omega_c}\right)^2}$$

$$\sigma = \frac{g\,\varepsilon_o}{\left(\frac{\omega}{\omega_c}\right)^2} \qquad 5.2$$

Cylindrical magnetron:

$$\varepsilon_{eff} = 1 - \frac{\rho_o \frac{e}{m} \varepsilon_o \left(1 \pm \sqrt{\frac{\omega_c \xi}{\omega}}\right)}{\omega_c \xi - \omega^2} \qquad 5.3$$

where $\xi = (\omega_c/2)(1 - \frac{r_c^2}{r^2})$

or, using the Hull-Brillouin relation for ρ_o :

$$\varepsilon_{eff} = 1 + \frac{\left(1 + \frac{r_c^4}{r^4}\right)\left(1 \pm \frac{1}{\sqrt{2}} \frac{\omega}{\omega_c} \sqrt{1 - \frac{r_c^2}{r^2}}\right)}{1 - \frac{r_c^2}{r^2} - 2\left(\frac{\omega}{\omega_c}\right)^2} \qquad 5.4$$

$$\sigma \cong g \varepsilon_o \frac{\frac{\omega_c^2}{2}\left[\frac{\omega_c^2}{2}\left(1 - \frac{r_c^2}{r^2}\right) + \omega^2\right] \pm \frac{\omega \omega_c^3}{\sqrt{2}} \sqrt{1 - \frac{r_c^2}{r^2}}}{\left[\frac{\omega_c^2}{2}\left(1 - \frac{r_c^2}{r^2}\right) - \omega^2\right]^2} \qquad 5.5$$

These last two relations are plotted in Figure 5.1 for $\frac{r_H}{r_c} = \infty$. It is seen that the maximum loss occurs in the vicinity of the singularity $\omega/\omega_c = 0.707$.

(b) Propagation normal to the anode and cathode:

Plane Magnetron:

$$\varepsilon_{eff} = 1 - \frac{1}{\left(\frac{\omega}{\omega_c}\right)^2} \qquad 5.6$$

$$\sigma = \frac{g \varepsilon_o}{\left(\frac{\omega}{\omega_c}\right)^2}$$

Cylindrical Magnetron:

$$\varepsilon_{eff} = 1 + \frac{1}{\omega^2} \frac{\rho_o e}{m \varepsilon_o} \left(1 + \frac{r_c^4}{r^4}\right) \frac{\frac{\rho_o e}{m \varepsilon_o}\left(1 + \frac{r_c^4}{r^4}\right) + \omega^2}{\omega^2 - \frac{\omega_c^2}{2}\left(1 - \frac{r_c^2}{r^2}\right) + \frac{\rho_o e}{m \varepsilon_o}\left(1 + \frac{r_c^4}{r^4}\right)} \qquad 5.7$$

or, using the Hull-Brillouin relations for ρ_o

$$\varepsilon_{eff} \cong 1 - \frac{\omega_c^2}{2\omega^2}\left(\frac{\omega^2 - \omega_c^2/2}{\omega^2 - \omega_c^2}\right) \qquad 5.8$$

$$\sigma \cong g\omega\varepsilon_o\left[\frac{1 + 2(\omega/\omega_c)^2}{1 - 2(\omega/\omega_c)^2} - \frac{7 - 8(\omega/\omega_c)^2 - \omega_c^2/2\omega^2}{4(1 - 2\omega^2/\omega_c^2)(1 - \omega^2/\omega_c^2)^2}\right] \qquad 5.9$$

for $r_c/r << 1$.

c. Discussion of the Results: Before proceeding with a presentation of the experimental data obtained, the preceding results will be discussed briefly.

The complex propagation constant has been found for an electromagnetic wave propagating through a magnetron-type space charge region without consideration of the attending circuit or boundary conditions which the wave must satisfy. It is proposed to make the analysis more complete by including the effects of the circuit into which the space charge is placed, in the near future. However, the results obtained to date will enable the effect of the space charge on certain types of circuit structures to be determined at least qualitatively.

The values of the propagation constant obtained have been expressed in terms of effective dielectric constant ε_{eff} and conductivity σ. The former is more interesting for the moment. Use of the concept of dielectric constant in this way should be interpreted as meaning only that a plane wave propagating in a particular direction (say along the y-axis) will travel with the same velocity in the space charge as in an ordinary dielectric of relative dielectric constant ε_{eff}. However, in

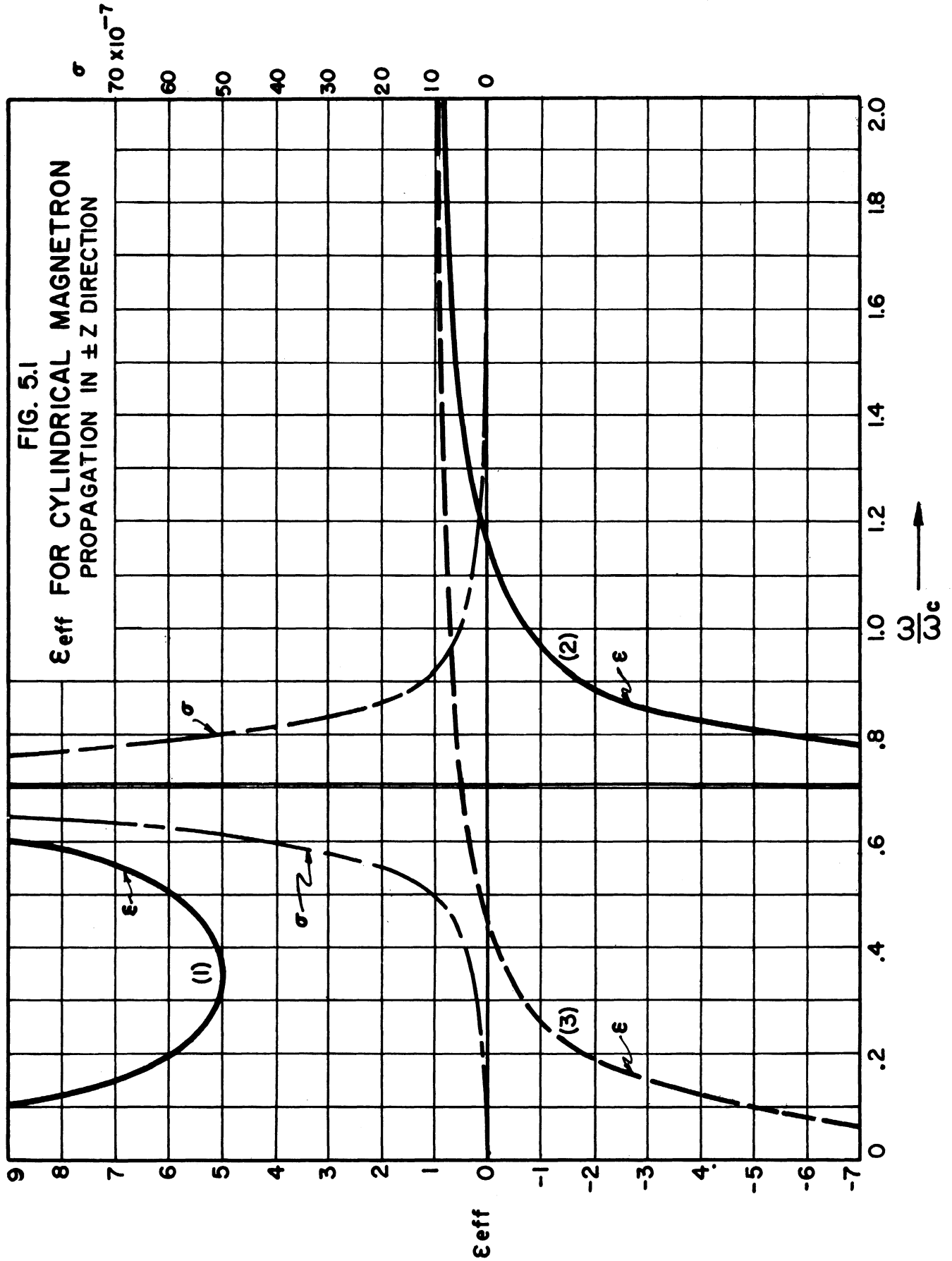
FIG. 5.1
εeff FOR CYLINDRICAL MAGNETRON
PROPAGATION IN ± Z DIRECTION
σ
70 x10⁻⁷
60
50
40
30
20
10
0
σ
(2)
ε
(1)
ε
σ
(3)
ε
9
8
7
6
5
4
3
2
1
0
-1
-2
-3
-4
-5
-6
-7
εeff
0
.2
.4
.6
.8
1.0
1.2
1.4
1.6
1.8
2.0
ω/ωc

general, the space charge is an anisotropic medium, so that great care must be exercised in the case where two waves are propagating in different directions.

The curves of Figure 5.1 show that the space charge can assume values of ϵ_{eff} which are positive, greater or less than unity, and negative. This latter means that the wave is effectively attenuated as it passes through the medium, and in this sense the space charge can be considered as behaving similarly to a conductor when $\epsilon_{eff} < 0$. In the region of positive dielectric constant less than unity, the phase velocity of the wave will of course exceed that of light, and the effect of this on the circuit must be examined in each individual case. In the region of positive dielectric constant greater than unity the space charge can be thought of as an ordinary dielectric.

B. Experimental Results

As explained in the previous progress report, a 10-cm resonant cavity magnetron diode has been constructed, of a design as shown in Figure 5.2, in order to obtain some indication as to the validity of the above mentioned thoery. This tube was completed and operated and data obtained which appear to confirm certain parts of the theory, but additional tests need to be made before anything can be stated with reasonable certainty.

Before considering the experimental data obtained, an examination of Figure 5.3, which is a plot of equation 5.4 for the value r_H/r_c used in the experiment, will enable a qualitative prediction to be made of what cavity resonant wave length shift is to be expected.

The experiment was conducted maintaining E_a/B^2 constant, so that presumably the cloud diameter was constant with a value $r_H = 3\ r_c$. Then as

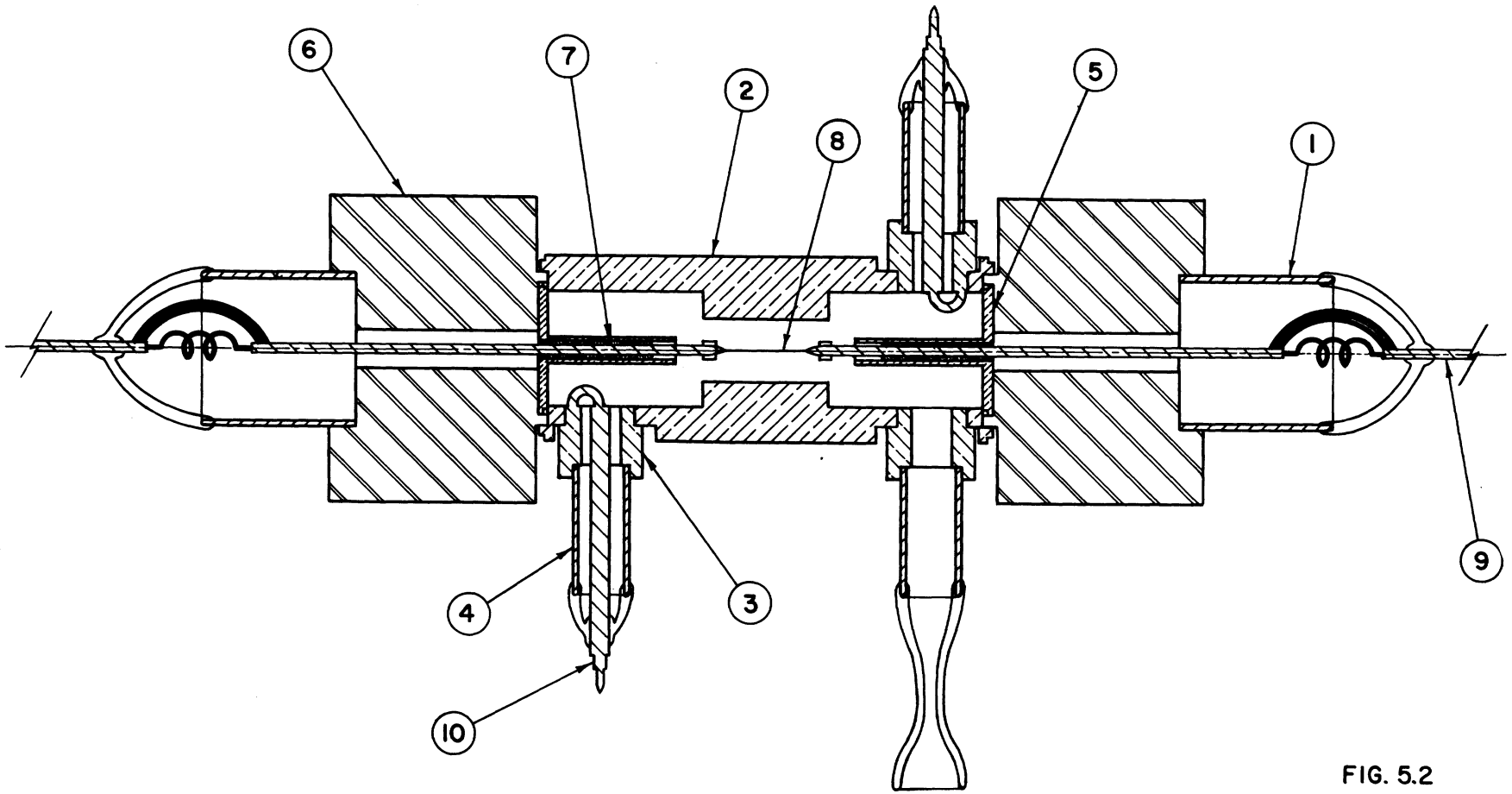

FIG. 5.2

ALL DIMENSIONS UNLESS OTHERWISE SPECIFIED MUST BE HELD TO A TOLERANCE - FRACTIONAL ± 1/64" DECIMAL ± .005" ANGULAR ± ½°

		ENGINEERING RESEARCH INSTITUTE UNIVERSITY OF MICHIGAN ANN ARBOR MICHIGAN	DESIGNED BY GPB	APPROVED BY
			DRAWN BY TT	SCALE
			CHECKED BY VPB	DATE 4-21-50
		PROJECT M-762	TITLE 10 CM MAGNETRON DIODE (EXPERIMENTAL) MODEL 3	
ISSUE	DATE	CLASSIFICATION	DWG. NO. B-11,003	

the applied magnetic field is raised (decrease ω/ω_c) the cloud exhibits a positive dielectric constant less than unity, so that the resonant wave length would be expected to decrease slightly. When $\omega/\omega_c = 1.115$, $\varepsilon_{eff} = 0$ and the space charge begins to behave slightly as a conductor, increasing the resonant wave length. As ε_{eff} becomes more negative the cloud behaves more and more as a conductor, so that the wave length should increase slowly after the first abrupt increase at $\omega/\omega_c = 1.115$. The reason an increase in negative ε_{eff} increases the similarity of the space charge to a conductor is, of course, that the effective attenuation is increased. For ω/ω_c slightly less than the singular value (.676) the dielectric constant changes to positive but is very great, so that no abrupt change in resonant wave length should be noted until ε_{eff} begins to decrease sharply (around $\omega/\omega_c = 0.6$) when it should decrease. The resonant wave length in the region $0.1 < \omega/\omega_c < 0.55$ should be relatively constant, less than the value in the range $0.6 < \omega/\omega_c < 1.115$, but greater than the value for $\omega/\omega_c > 1.115$. For $\omega/\omega_c < 0.1$, there should again be an abrupt increase in λ_o.

The reasons for the above predictions of wave length shift can be seen most easily by considering a simple example. The condition for resonance in an open length ℓ of coaxial transmission line shorted on one end is

$$\beta \ell = \pi/2$$

where $\beta = 2\pi\eta/\lambda_o$. η is the ratio of velocity of propagation of the wave along the line to the velocity of light. An increase in ε_r for a dielectric cylinder surrounding a part of the length of the center conductor (at the open end) will increase η and vice versa. Thus, for

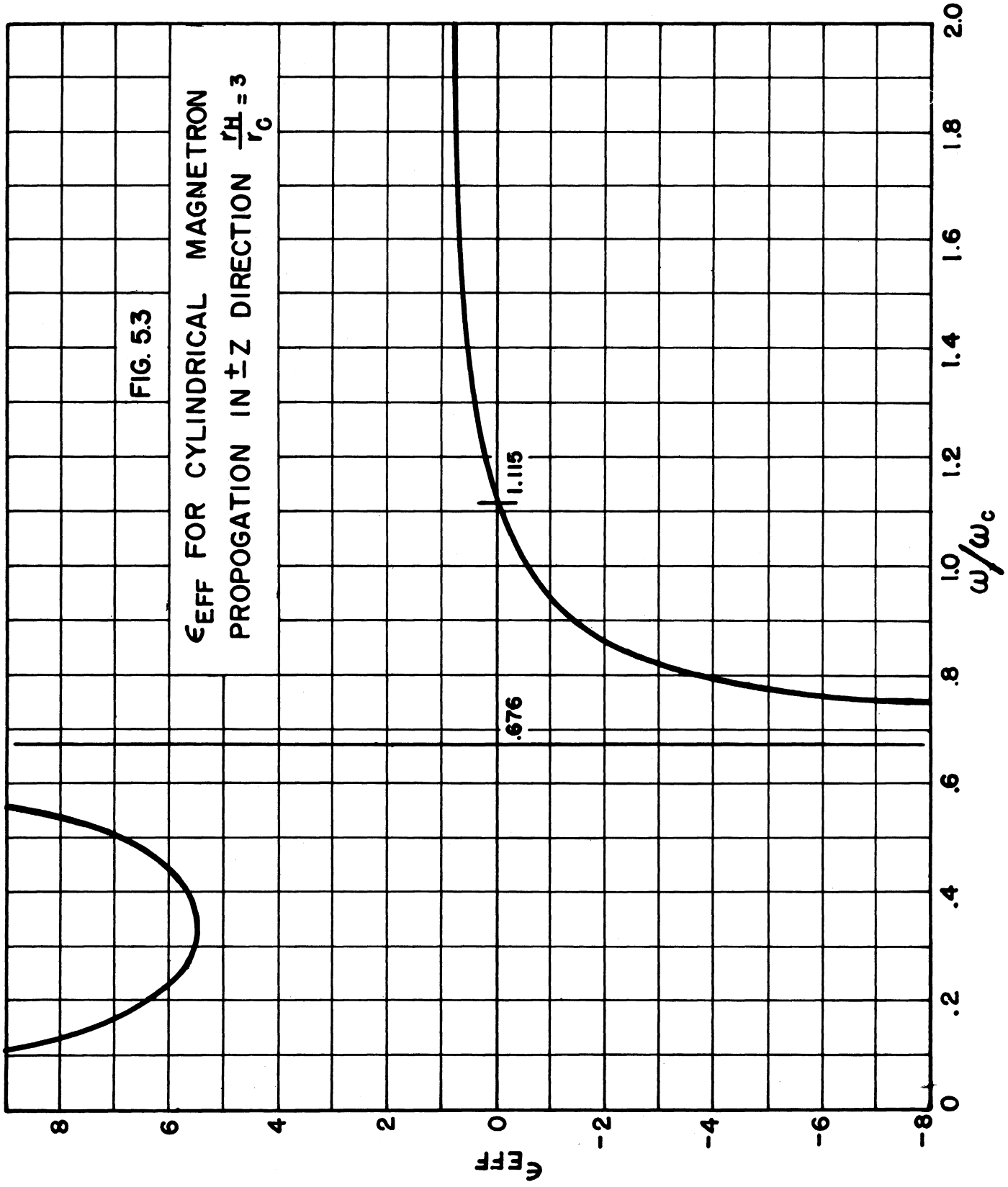
FIG. 5.3
ϵ_{EFF} FOR CYLINDRICAL MAGNETRON
PROPOGATION IN ±Z DIRECTION $\frac{r_H}{r_c} = 3$
ϵ_{EFF}
8
6
4
2
0
-2
-4
-6
-8
.676
1.115
0
.2
.4
.6
.8
1.0
1.2
1.4
1.6
1.8
2.0
ω/ω_c

$0 < \varepsilon_{eff} < 1$, $0 < \eta < 1$ and $\lambda_o = 4\ell\eta$ will decrease; while for $\varepsilon_{eff} > 1$, λ_o will increase. If $\varepsilon_{eff} < 0$ the space charge can be considered as increasing the diameter of the inner conductor, thus increasing the resonant wave length.

The data obtained from the tube shown in Figure 5.2 are plotted in Figure 5.4. The resonant wave length of the cavity remains relatively constant as the applied magnetic field is increased (ω/ω_c decreased) until $\omega/\omega_c \cong 1.4$, when it rises, reaching a reasonably constant value and dropping again very abruptly at $\omega/\omega_c = 0.63$. The two curves are believed due to two resonances in the cavity. Both exhibit the same general behavior as far as the discontinuities are concerned.

The sharp drop at $\omega/\omega_c = 0.63$ is regarded as confirmation of the analytical method followed, as outlined in the previous progress report. This follows from the fact that the angular velocity of an electron in a magnetron results from the integral of the angular equation of motion with only the assumption of zero angular velocity at the cathode. The value of the angular velocity, unlike the potential or space charge density, does not depend on any choice or assumption regarding the electronic orbit, or on a series solution. Therefore, the angular velocity is believed to be invarient under any changes in emission, charge density, voltage, etc., and since the position of the singular value of ω/ω_c is, from the above theory, governed entirely by the functional dependence of the angular velocity on radius, this agreement between Figure 5.4 and 5.3 is thought to be significant.

The situation regarding the increase in $\Delta\lambda$ at $\omega/\omega_c = 1.4$ does not agree with that predicted from Figure 5.3. This will be discussed below and some possible explanations of the disagreement advanced.

From equation 5.3 it is seen that the value of ω/ω_c for $\mathcal{E}_{eff} = 0$ is a function of the radius of the cloud, the space charge density at the edge of the cloud, and the applied magnetic field. If the well-known equation for the radius of the cloud (equation 5.13, Technical Report No. 1) is valid, the only variable is ρ_o. Thus, if the abrupt increase in λ_o at $\omega/\omega_c = 1.4$ is interpreted as the point $\mathcal{E}_{eff} = 0$, we can solve equation 5.3 for ρ_o to obtain ($\omega/\omega_c = 1.4$)

$$\frac{\rho_o e}{m\mathcal{E}_o} \cong - \omega_c^2$$

whereas the Hull-Brillouin relation would give

$$\frac{\rho_o e}{m\mathcal{E}_o} = - \frac{\omega_c^2}{2}$$

This value, greater than that given by the Hull-Brillouin solution, is slightly surprising and reminds one of the solutions of Page and Adams[3] and Moeller[4] who found that ρ_o increases abruptly at the edge of the space charge swarm.

The above interpretation of the increase in $\Delta\lambda$ at $\omega/\omega_c = 1.4$ of Figure 5.4 should not be considered as final, however, since the experimental conditions of the space charge cloud were far from ideal. The principal possible source of error lies in the formation of the space charge cloud. The magnetic circuit used apparently made the production of an absolutely uniform magnetic field impossible, so that there will

---

[3]Page and Adams, Phys. Rev., Vol. 69, p. 494, 1946.

[4]Moeller, H. G., Hoch freq. und Elak., Vol. 47, p. 115, 1936.

FIG. 5.4
CHANGE IN RESONANT WAVELENGTH OF 10 CM. CAVITY vs ω/ω_c

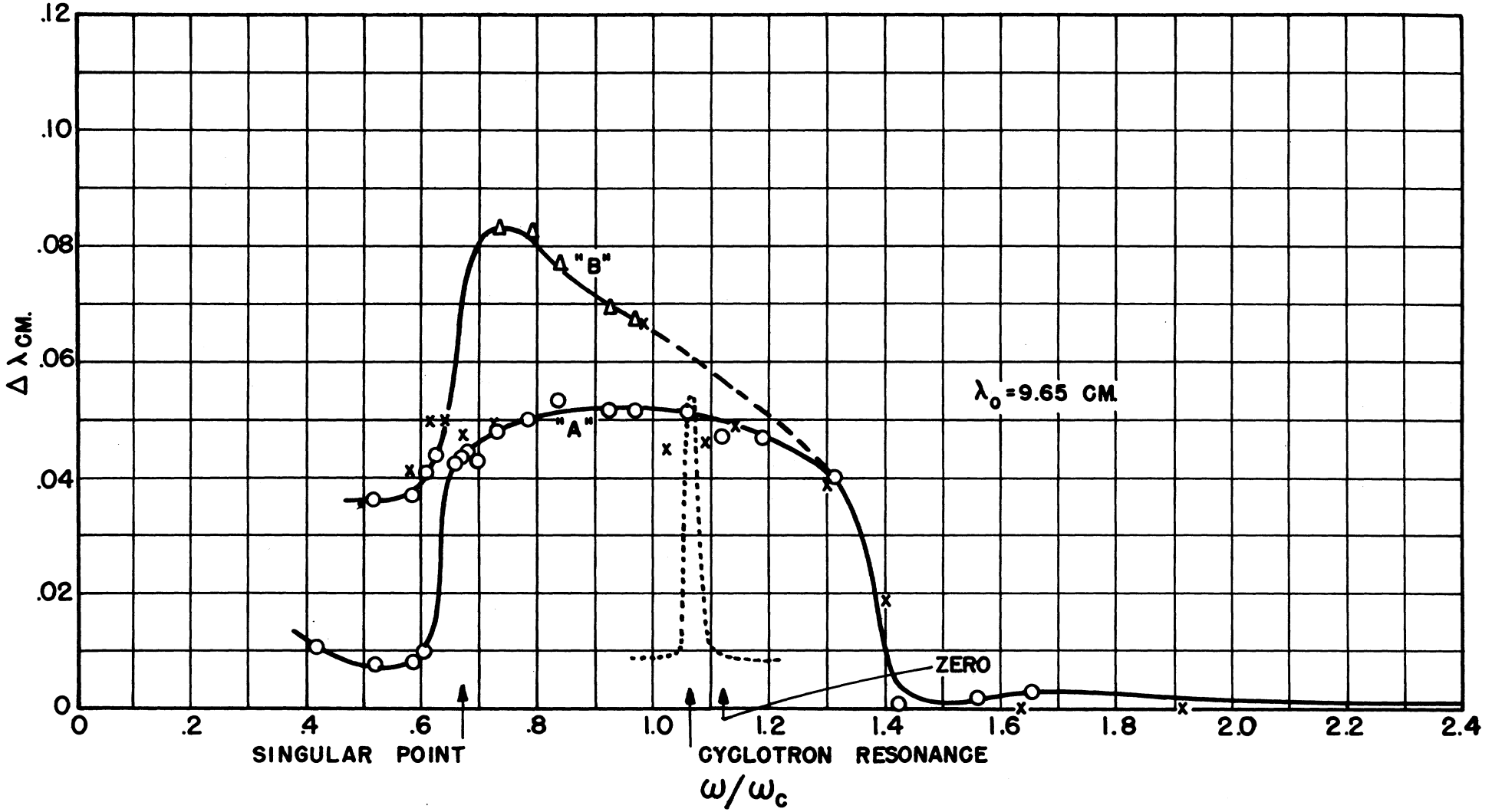

PG. 89
BK. 6
G.R.B

FIG. 5.5
CHANGE IN RESONANT WAVELENGTH OF 10 CM. CAVITY
vs. MAGNETIC FIELD - SHOWING THE CYCLOTRON RESONANCE

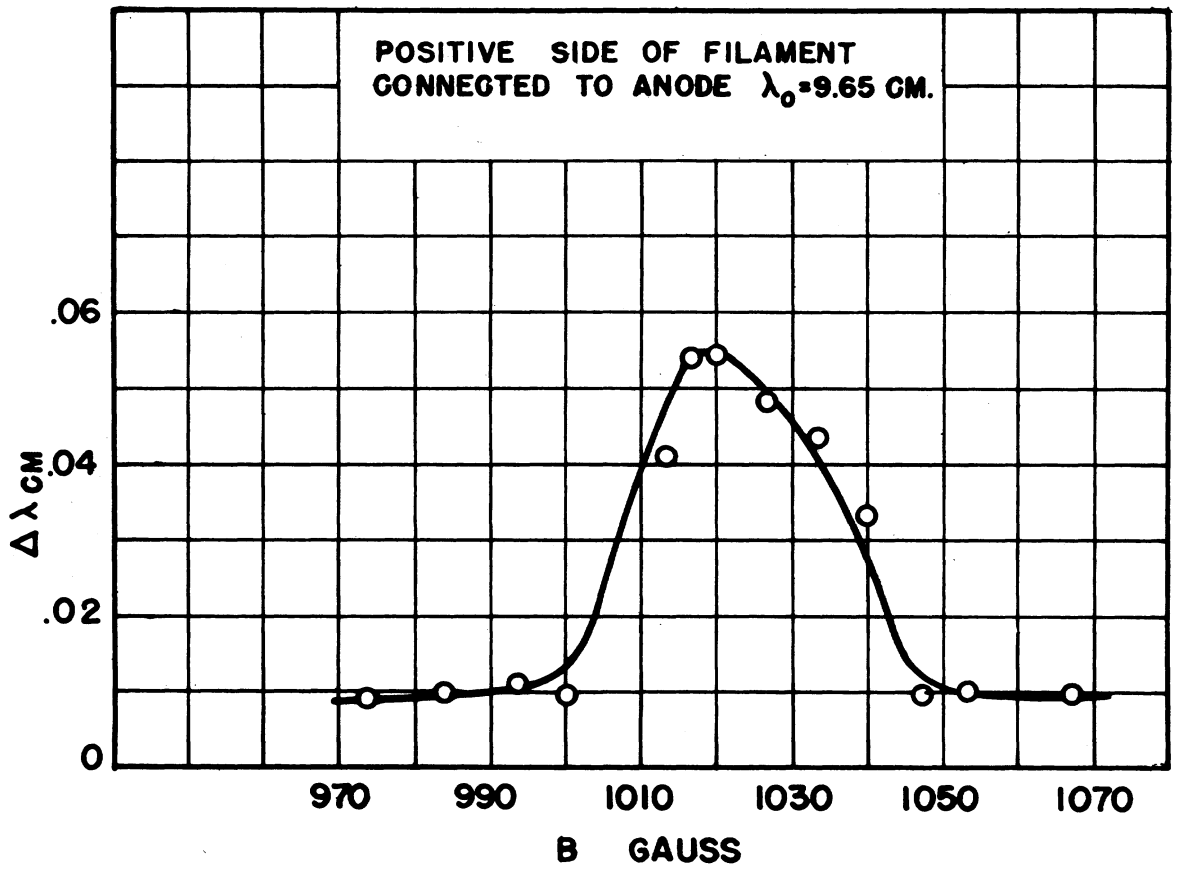

PG. 91
BK. 6
G.R.B

be a longitudinal force[5]

$$F_z = - \frac{re}{2} \sqrt{\frac{2W_\perp}{m}} \frac{\delta H}{\delta z}$$

where r is the radius of the electron orbit, $W_\perp$ its kinetic energy in the plane perpendicular to the z-axis and H the magnetic intensity. Thus electrons can move axially from the filament under the influence of the above force. In operation such current was observed, constituting about one-fourth of the emission current for high anode voltages. It would be expected that this drain of current would affect the composition of the space charge cloud. A calculation of the wave length shift for the case $\varepsilon_{eff} = 8$ ($\omega/\omega_c = 0.4$) yielded a value greater than the observed by a factor of ten, indicating that the cloud is probably much smaller (probably shorter) than believed, but the sharp rise and fall of the $\Delta\lambda$ characteristic is an indication that at least part of the cloud is of the form expected.

The shift in resonant wave length of the cavity was observed as a function of magnetic field in the vicinity of the cyclotron field (calculated 1060 gauss) and is shown in Figures 5.4 and 5.5. This observation was made with the positive side of the filament connected to the anode, no shift in wave length being observed when the negative side of the filament was connected to the anode. It is noted that the wave length shift maximum occurs at a value of ω/ω_c about seven percent greater than unity, indicating a probable error in magnet calibration or residual magnetism effect in the cyclotron resonance test. A search was made to try to

---

[5] See, for example, Alfven, "Cosmical Electrodynamics", Oxford, 1950, p. 19.

detect any shift in the negative direction (decrease in λ_o) without success.

The tests on this tube will be continued after insertion of a new straightened filament.

6. LOW POWER MAGNETRON FOR LOW Q OPERATION -- (J. S. Needle)

The Model 9 magnetron consists of an anode structure contained in an evacuated glass-sealed envelope. It is to be used in an externally tunable coaxial line and serves only as the capacitive portion of the resonant circuit. The capacitive section consists of six radial vanes attached to an outer cylinder which extend through 6 longitudinal slots in an inner cylinder. Thus a 12-anode set is formed with dimensions based on an interaction space design for 10 cm. The cathode is of the standard nickel-based oxide-coated mesh type. A sketch of the Model 9 magnetron appears on page 46, Figure 7.1 of the second quarterly progress report for this project.

Assembly of the Model 9 magnetron reached the pump out stage, at which a leaky butt seal between the glass and one of the Kovar cups was encountered (See Figure 7.1 of Quarterly Report No. 2). Attempts to repair this seal resulted in the fracture of the glass seal at the opposite end of the outer anode. Initially, the sealing operations between the inner and outer anodes were completed only after several unsuccessful attempts. This difficulty has been attributed to the longitudinal differential expansion between the inner and outer anode components.

In order to overcome the glass sealing problem, the Model 9 design has been modified and has been designated Model 9A. A sketch of Model 9A appears in Figure 6.1. The outer anode ring of the Model 9A consists of a Kovar cylinder to which the vane anodes are brazed. The inner anode of the Model 9A differs from the Model 9 in that a sliding fit between one end of the copper portion of the

inner anode and its connecting Kovar cylinder is employed to overcome the effects of differential expansion.

Parts for the Model 9A magnetron have been completed and are now in the process of assembly. A small change in the inner anode tooth design along with the modifications mentioned above has resulted in a considerable reduction in fabrication time.

The problem of leakage of r-f power through the cathode line will initially be dealt with by using a choke and by-pass system designed for 10 cm. Modifications for broad banding in the cathode line will be investigated after a workable magnetron at 10 cm has been produced.

An investigation of the circuit properties of the coaxial line type resonator, of the type to be used with this tube, and associated lumped constant appendages has been started and to date shows promise as a guide to the understanding of shunt impedance.

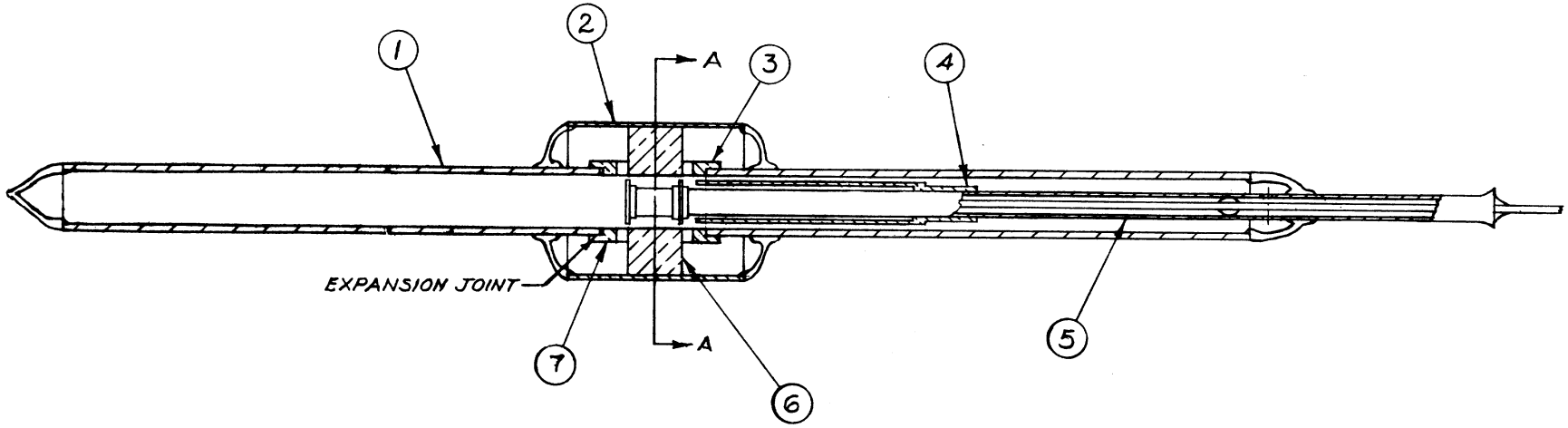

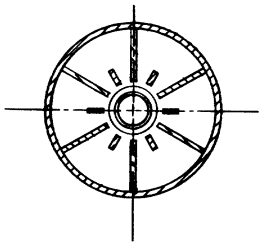

SECTION A A

FIG. 6.1

ALL DIMENSIONS UNLESS OTHERWISE SPECIFIED MUST BE HELD TO A TOLERANCE - FRACTIONAL ± 1/64" DECIMAL ± .005" ANGULAR ± ½°

ENGINEERING RESEARCH INSTITUTE UNIVERSITY OF MICHIGAN ANN ARBOR MICHIGAN		DESIGNED BY J.S.N	APPROVED BY
		DRAWN BY T.T.T	SCALE 2X
		CHECKED BY R.W.W	DATE 9-18-50
PROJECT M-762		TITLE LOW POWER MAGNETRON MODEL 9A	
CLASSIFICATION		DWG. NO. B-10,009A	
ISSUE	DATE		

7. MODEL 6 F-M MAGNETRON -- (H. W. Welch, Jr.)

The Model 6 f-m magnetron has a coaxial resonant cavity, two anode sets, and two cathodes. There are sixteen anodes in the oscillator section and four in the modulator section. Resonant wave length in the desired mode is 13 centimenters. For this mode, the coaxial cavity is one wave length long with a voltage maximum at each anode set. An assembly drawing is shown in Figure 10.1 of Quarterly Progress Report No. 2. Five of eight tubes built have been operated. Modulation data have been obtained on two of these.

The Model 6 No. 31, f-m magnetron was rebuilt during this period without successful results. Satisfactory operation could not be obtained without removing the modulator. The last change was to make the by-pass capacitance in the cathode structure as large as possible. Before going further with the Model 6 it seems advisable to solve this cathode problem by making cold measurements on non-operating models and by working with the Model 7 tube, which is simpler in construction than the Model 6.

8. MODEL 8 RECTANGULAR TUBE -- (J. R. Black)

The Model 8 rectangular tube was conceived as a structure adaptable to f-m use. A photograph and drawing of Model 8 are shown in Figures 8.1 and 8.2. It is essentially a capacity-loaded full wave length cavity having two sets of interdigital anodes each placed at a voltage maximum. The structure would form an f-m magnetron if one set of anodes were designed as an oscillating magnetron and the other set designed to form a variable reactance. It is apparent that the power output of such a structure having both sets of anodes designed as oscillating magnetrons would be considerably greater than that derived from a single cathode structure. It is believed that extremely high power magnetrons might be developed by lengthening the cavity and employing several sets of anodes and cathodes.

The cold testing of the Model 8 type structure was discussed in an earlier report (see section II C of Quarterly Report No. 1) in which a brass model was studied having anodes of the type used in the Model 4 magnetron. Based on this study a hot model was built with, however, a changed anode design for more efficient operation. The frequency was scaled to 13 cm. Both sets of anodes were designed as oscillators so as to be able to study the parallel operation of the sets of anodes as well as the f-m features.

Due to the fact that probes could not be inserted within the hot model to determine the exact mode of operation, it was most difficult to cold test the tube before the cathodes were sealed. The chokes were therefore designed to operate at the expected 13 cm. Two output loops were used to facilitate cold tests.

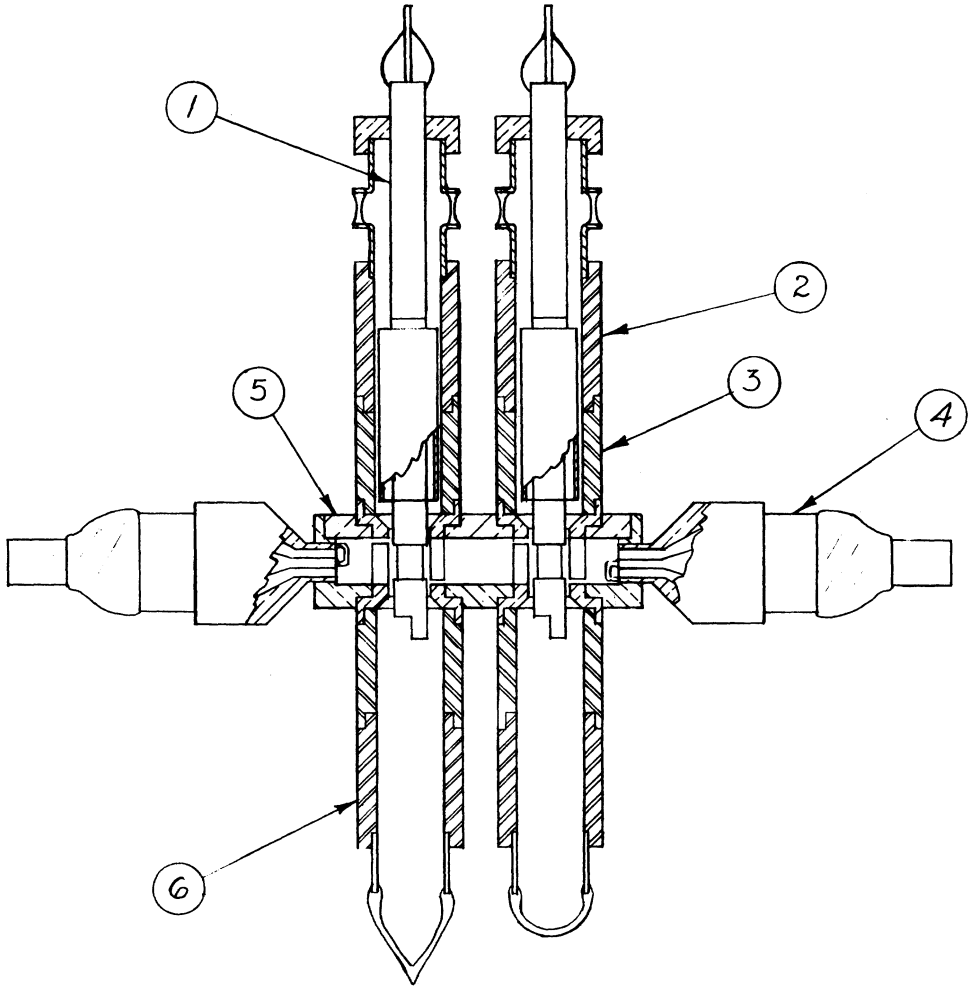

FIG. 8.1

ALL DIMENSIONS UNLESS OTHERWISE SPECIFIED MUST BE HELD TO A TOLERANCE - FRACTIONAL ± 1/64" DECIMAL ± .005" ANGULAR ± ½°

ISSUE / DATE	ENGINEERING RESEARCH INSTITUTE UNIVERSITY OF MICHIGAN ANN ARBOR MICHIGAN	DESIGNED BY J.R.B., H.W.W	APPROVED BY
		DRAWN BY N.N	SCALE FULL
		CHECKED BY H.W.W	DATE 9-15-50
	PROJECT M-762	TITLE DOUBLE ANODE MAGNETRON	
	CLASSIFICATION	DWG. NO. B- 10.008	

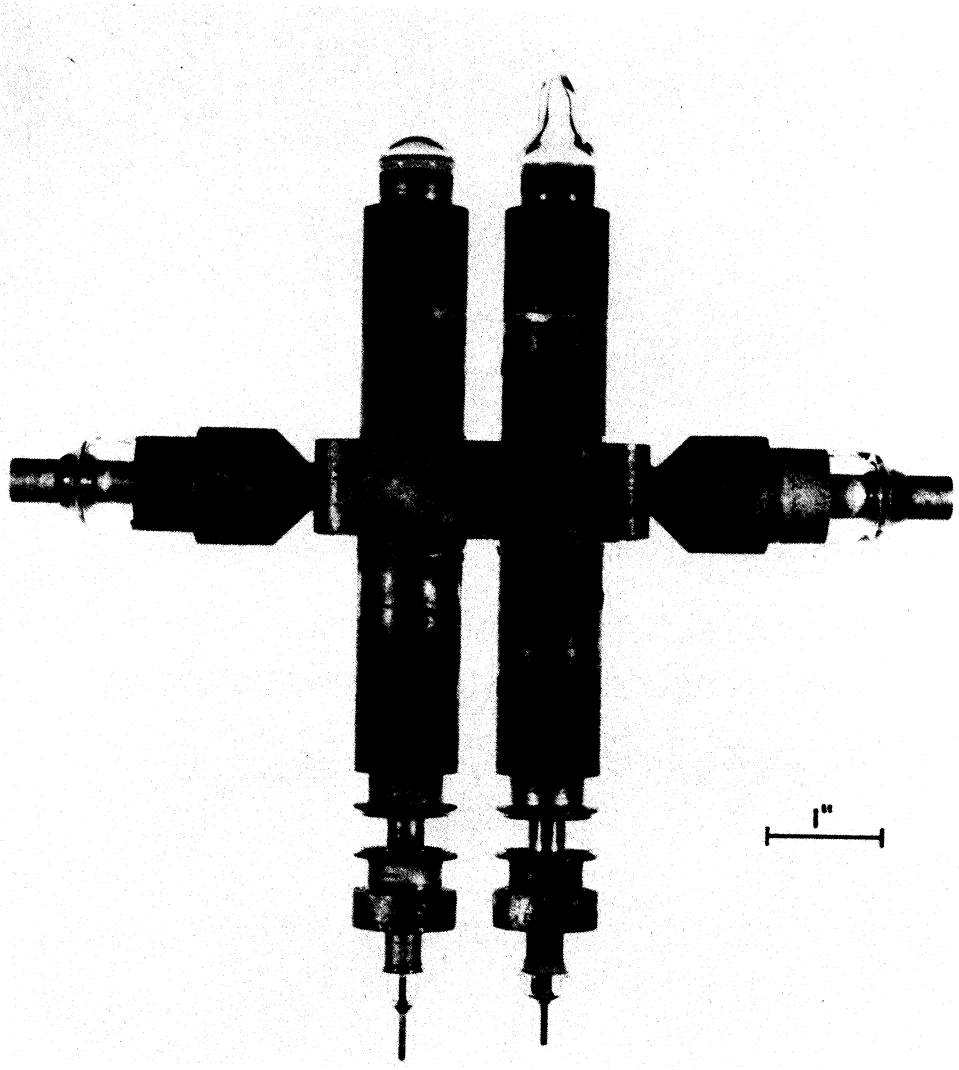

FIG. 8.2
MODEL 8 NO. 36 DOUBLE ANODE MAGNETRON

The following are the design parameters used for Model 8:
(See Figure 8.6 for symbols)

r_a	.45 cm	cavity	3 x 6 cm
r_c	.30 cm	h	1.02 cm
$\frac{r_a}{r_c}$	1.5	ℓ	.90 cm
		d	.089 cm
L	.724	N	16
R_a	.762	C_A	4 $\mu\mu$f

Preliminary examination of the operating model indicates clearly that two sets of anodes lock in on the same frequency and the power input to the structure is approximately double that of a single tube. Figures 8.3, 8.4 and 8.5 show voltage-current curves of the tube for three different magnetic fields under pulsed conditions. Curves are plotted for each cathode operating individually as well as both of them operating in parallel. These curves were taken from an oscilloscope with the voltage scale approximately 330 volts per division. Figure 8.6 is a voltage-current plot for a tube operating in a magnetic field corresponding to that in Figure 8.3. All of the above curves were taken with a load placed only on one of the two output connections.

As yet no attempt has been made to identify the various modes of operation; however, extensive study of this tube is being planned for the immediate future including f-m as well as the parallel operation.

At this early date it appears that this type of structure holds great promise for the development of high powered magnetrons.

A geometry consisting of a wave guide bent around to form a ring having several sets of anodes and cathodes would probably be a desirable form for a higher powered tube.

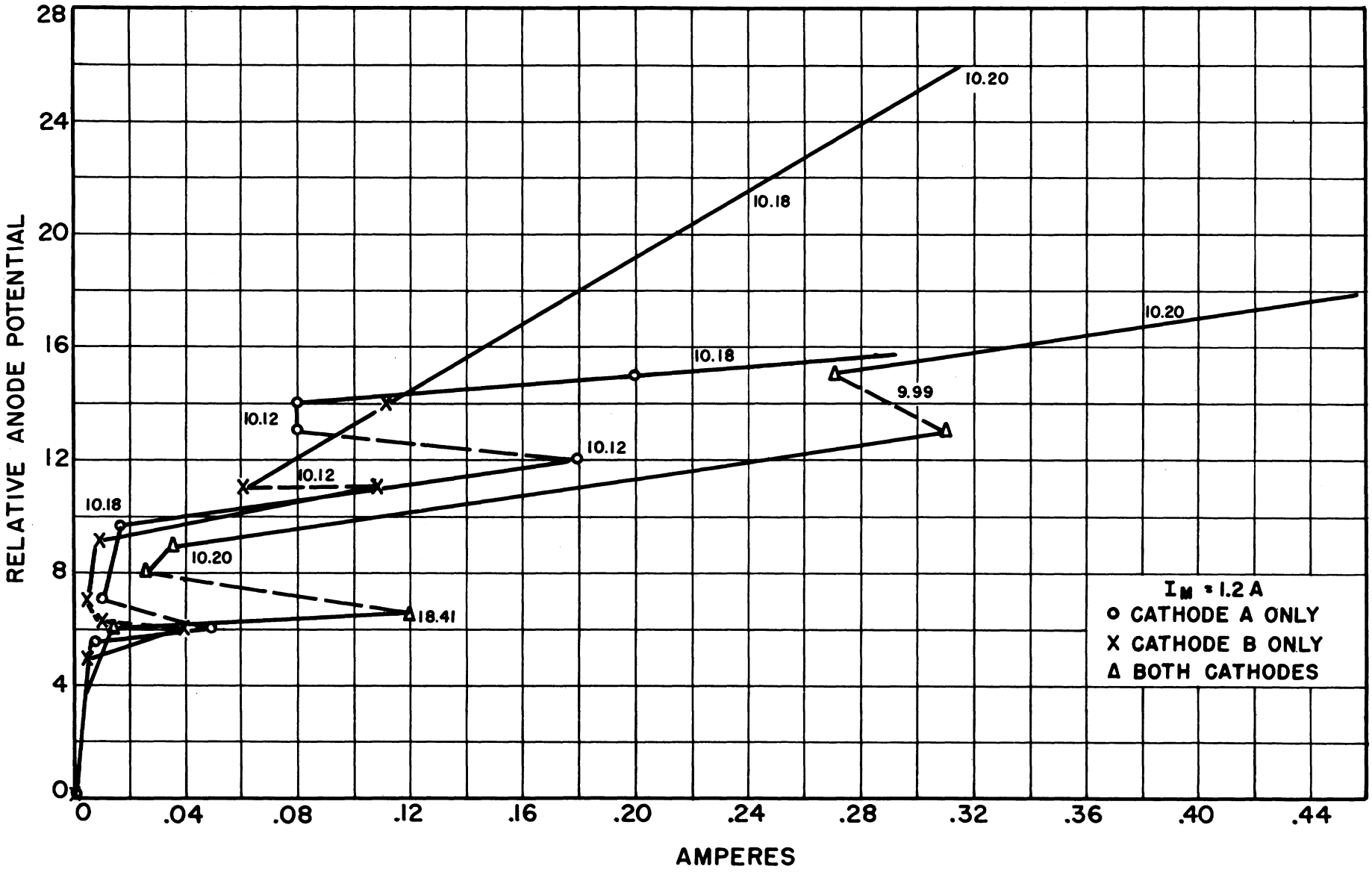

FIG. 8.3

PERFORMANCE CHARACTERISTICS MODEL 8 #36 (PULSED)

FROM OSCILLOSCOPE SCREEN, VERTICAL SCALE APPROX. 330 V/UNIT

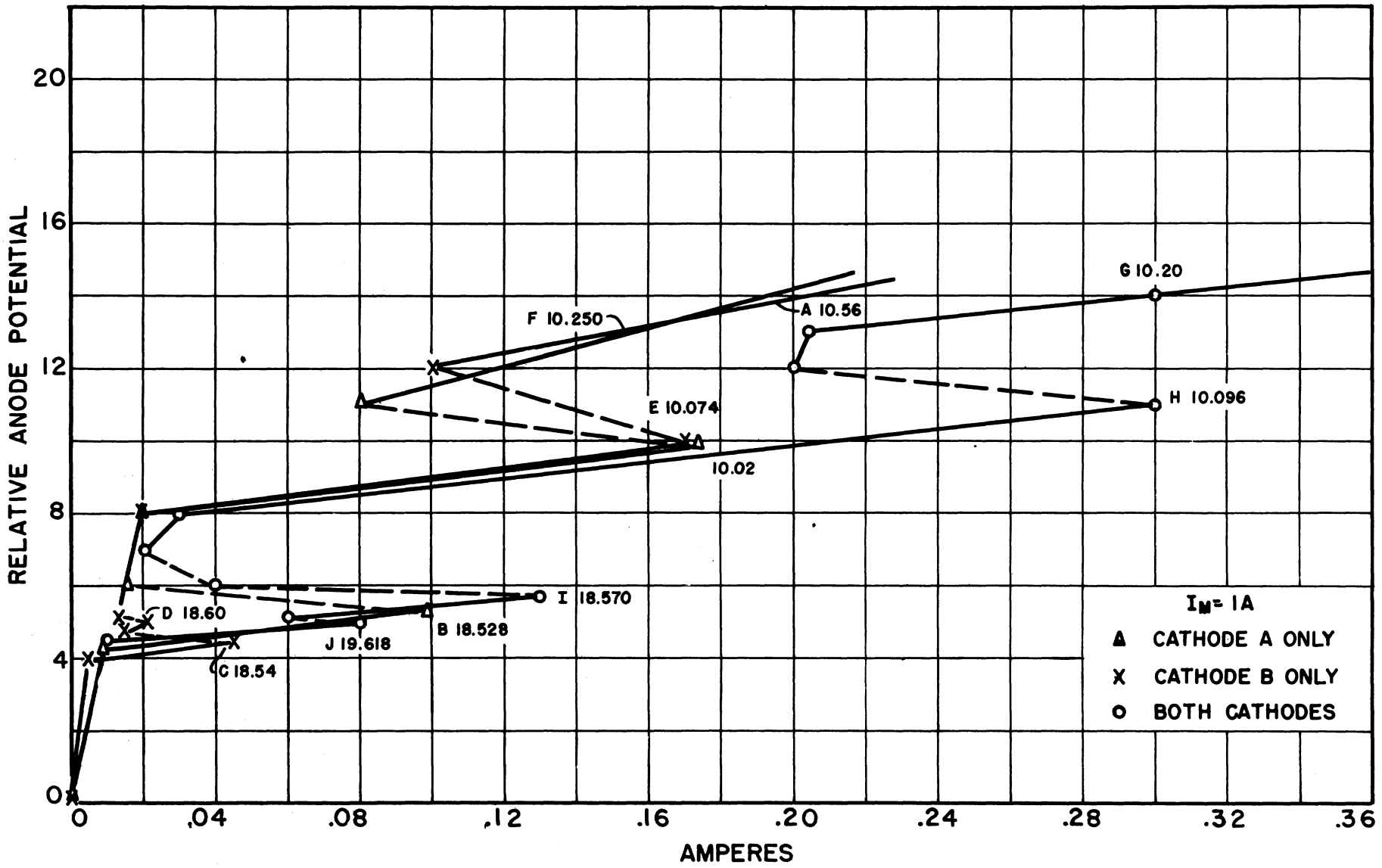

FIG. 8.4

PERFORMANCE CHARACTERISTICS MODEL 8 #36 (PULSED)

FROM OSCILLOSCOPE SCREEN. VERTICAL SCALE APPROX. 330 V/UNIT

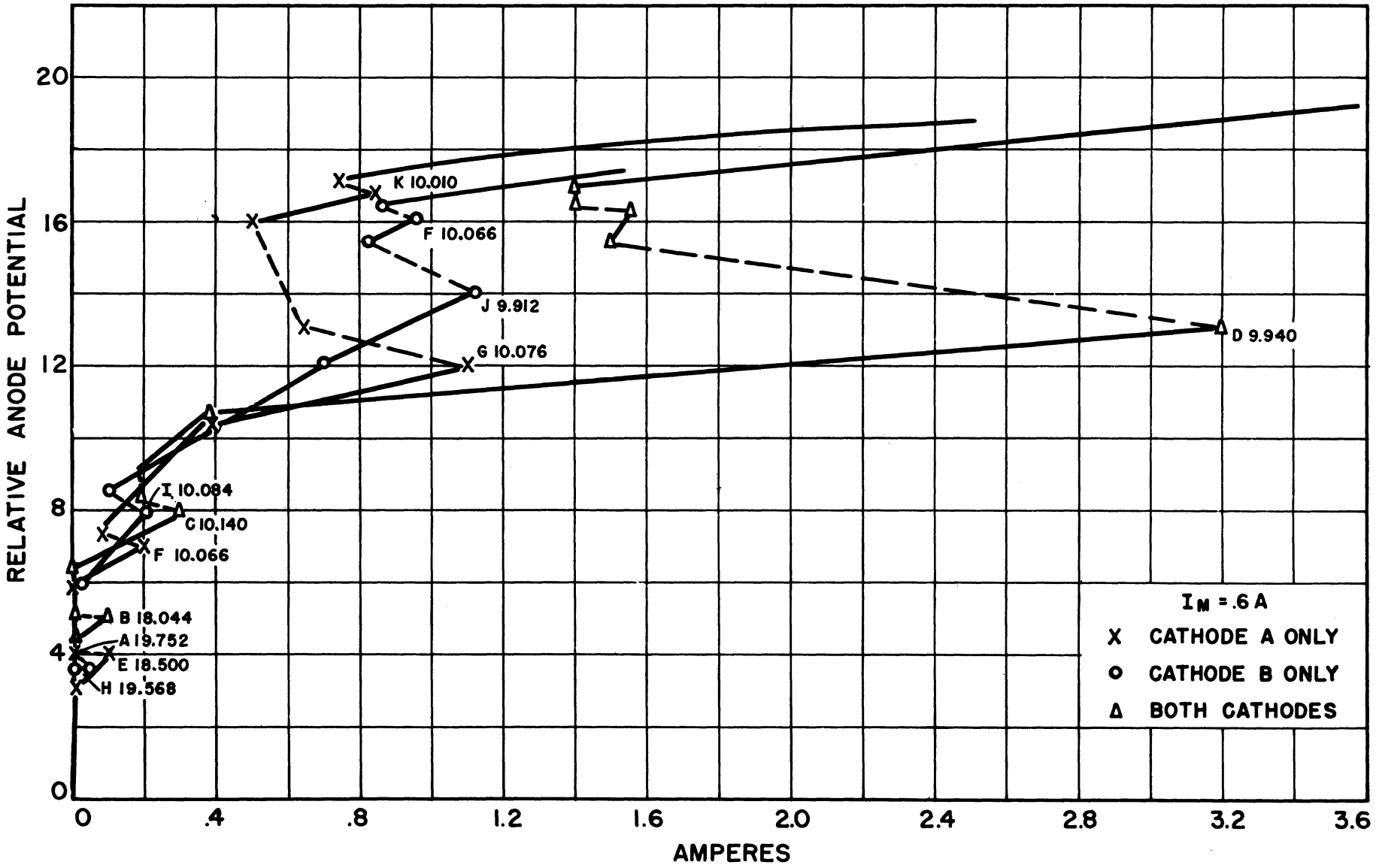

FIG. 8.5
PERFORMANCE CHARACTERISTICS MODEL 8 #36 (PULSED)
FROM OSCILLOSCOPE SCREEN. VERTICAL SCALE APPROX. 330 V/UNIT

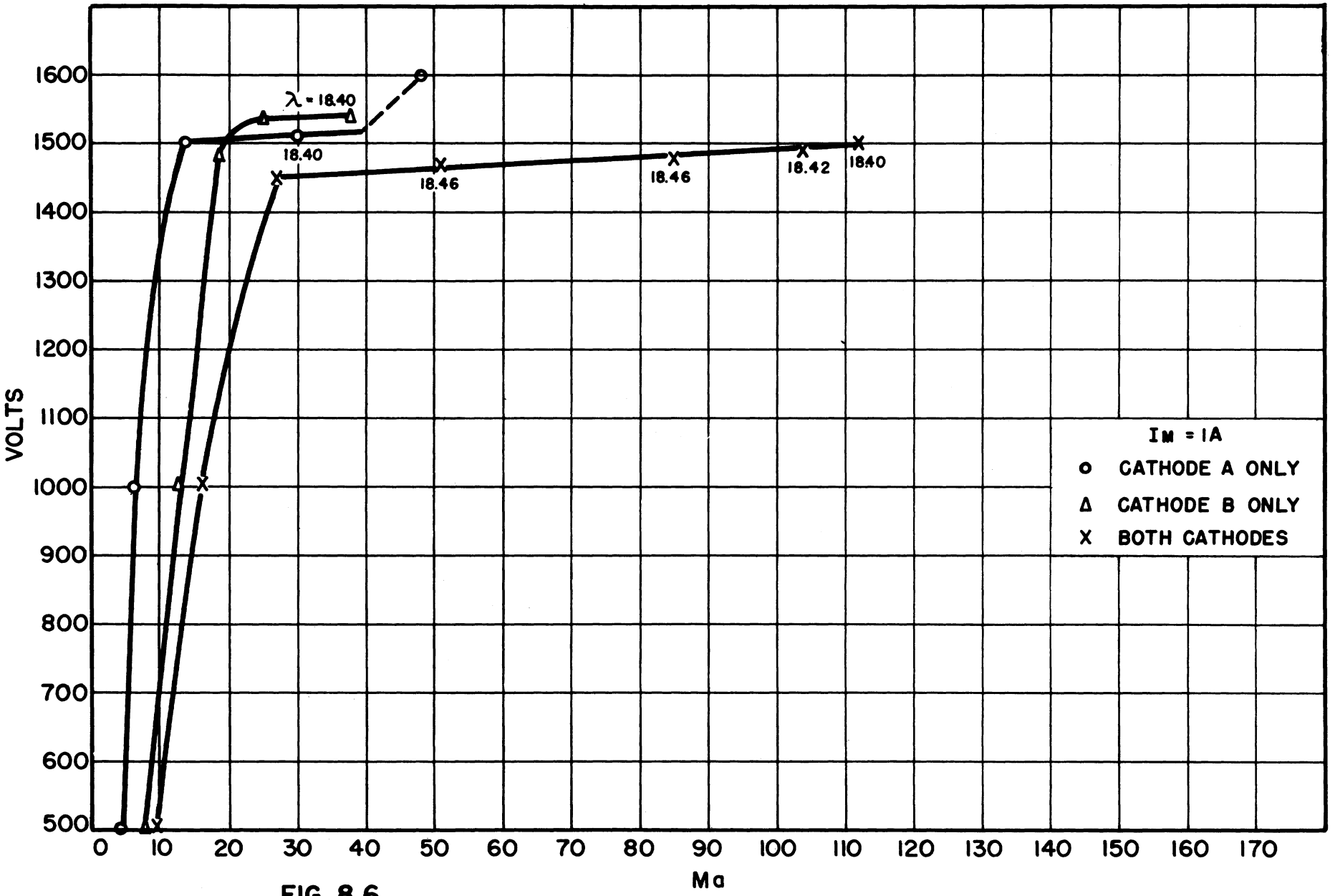

FIG. 8.6
PERFORMANCE CHARACTERISTICS MODEL 8 #36,

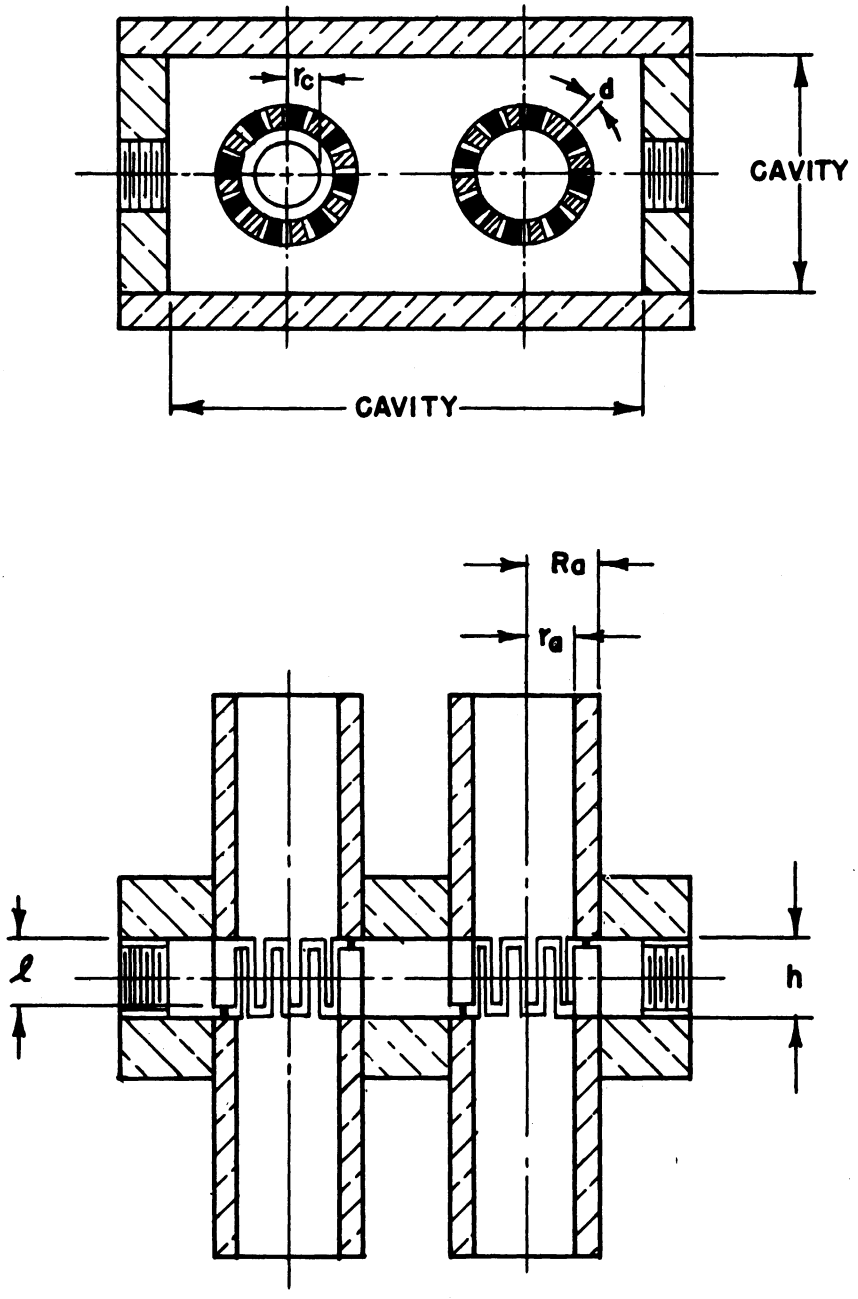

FIG. 8.7
SKETCH OF MODEL*8 MAGNETRON

9. THE TRAJECTRON, AN EXPERIMENTAL MAGNETRON DIODE -- (W. Peterson)

The purpose of this experiment is to attain a more complete understanding of the magnetron by studying the space charge in a smooth bore D. C. magnetron. A tube has been designed in which an electron beam can be sent through the space charge axially. The beam will start out grazing the cathode. Its exit point will be shown on a fluorescent screen. By varying the beam velocity, it should be possible to determine the path of an individual electron for a particular anode potential and magnetic field. This tube has been named the trajectron.

During the past period the construction of the trajectron has been carried up to the point where it is ready to be pumped out, and at the time of the writing of this report it is on the vacuum pump. With good fortune, the tube should be in operation within a week.

Photographs of the tube are shown in Figures 9.1 and 9.2 and a section drawing appears as Figure 9.3. A detail of the cathode section is shown in Figure 9.4. All glassing operations were done in a lathe. The tube was made in two halves, and then the final operation was the brazed joint at the electron gun end of the bellows, for which "BT" solder was used. All other brazed joints use gold-copper solder.

In assembling the diode section, the cathode and the anode were placed each in one end of the lathe. They were lined up with an indicator, then glassed together. Then the chuck was removed from the anode end and the markings were put on the outside

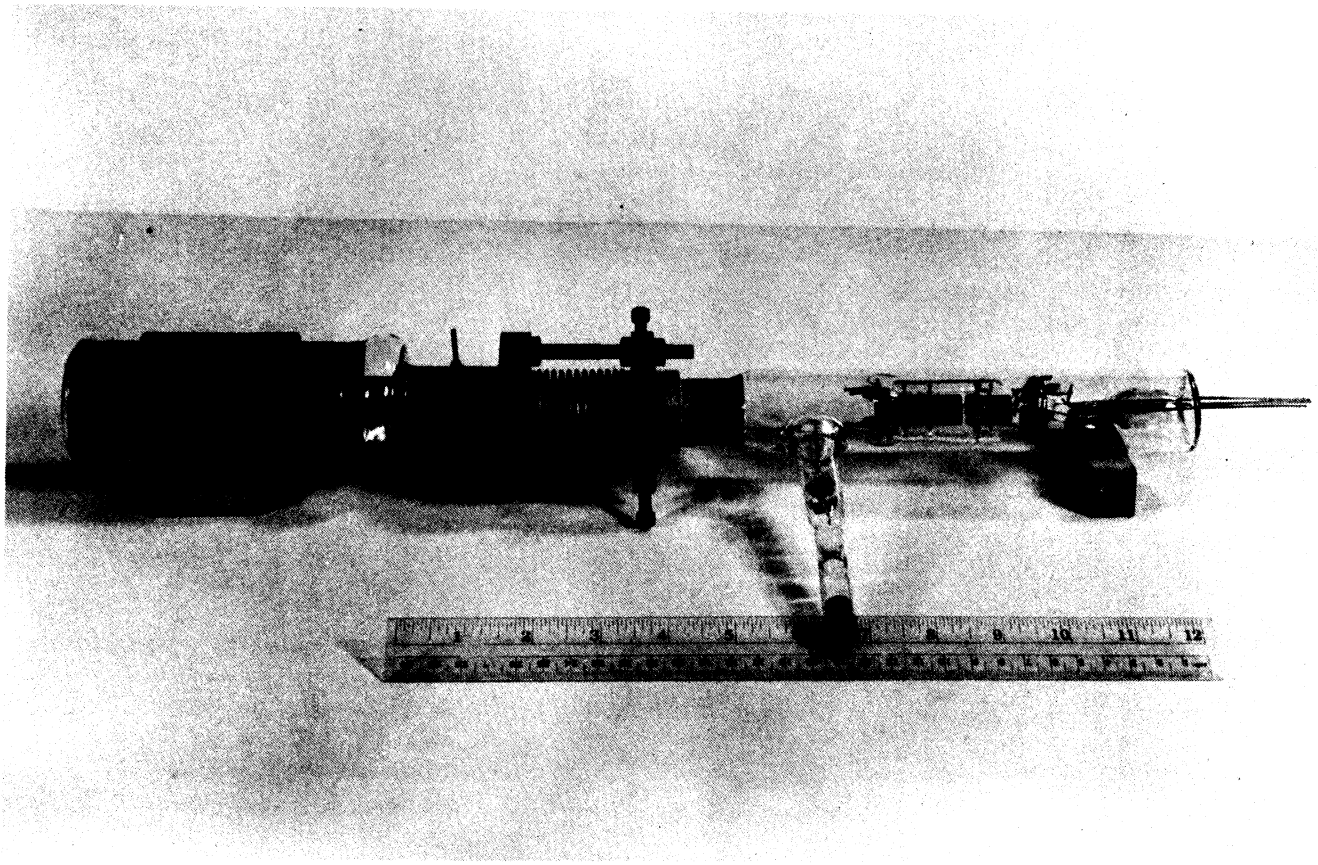

FIG. 9.1
OVERALL VIEW OF ASSEMBLED TRAJECTRON

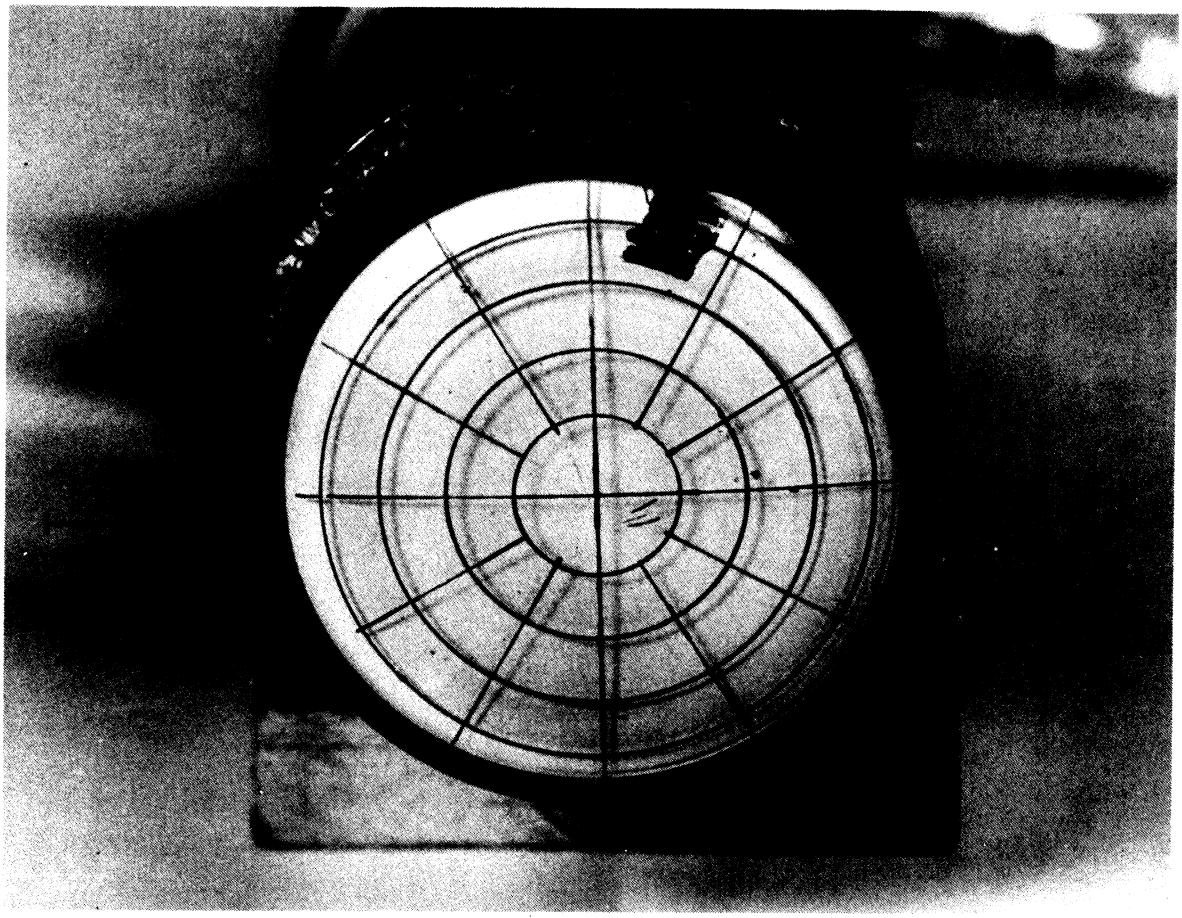

FIG. 9.2
VIEW SCREEN OF TRAJECTRON

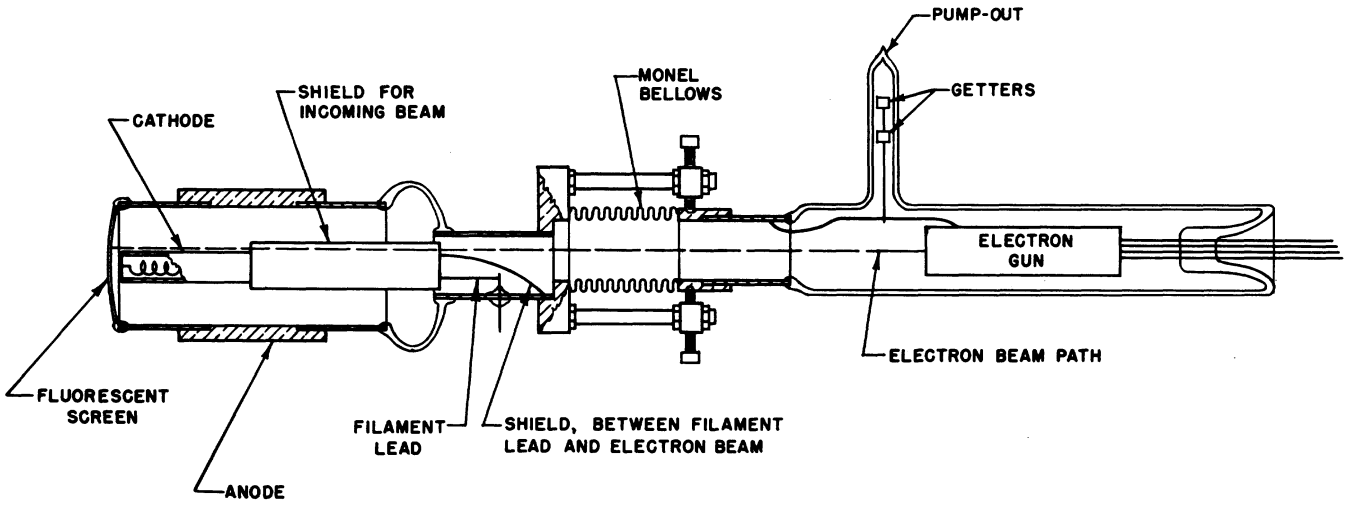

FIG. 9.3

ALL DIMENSIONS UNLESS OTHERWISE SPECIFIED MUST BE HELD TO A TOLERANCE - FRACTIONAL ± 1/64" DECIMAL ± .005" ANGULAR ± 1/2°

		ENGINEERING RESEARCH INSTITUTE UNIVERSITY OF MICHIGAN ANN ARBOR MICHIGAN	DESIGNED BY WP, HWW	APPROVED BY
			DRAWN BY TTT	SCALE 1/2
			CHECKED BY HWW	DATE 9-20-50
		PROJECT M-762	TITLE TRAJECTRON	
ISSUE	DATE	CLASSIFICATION	DWG. NO. B-11,004	

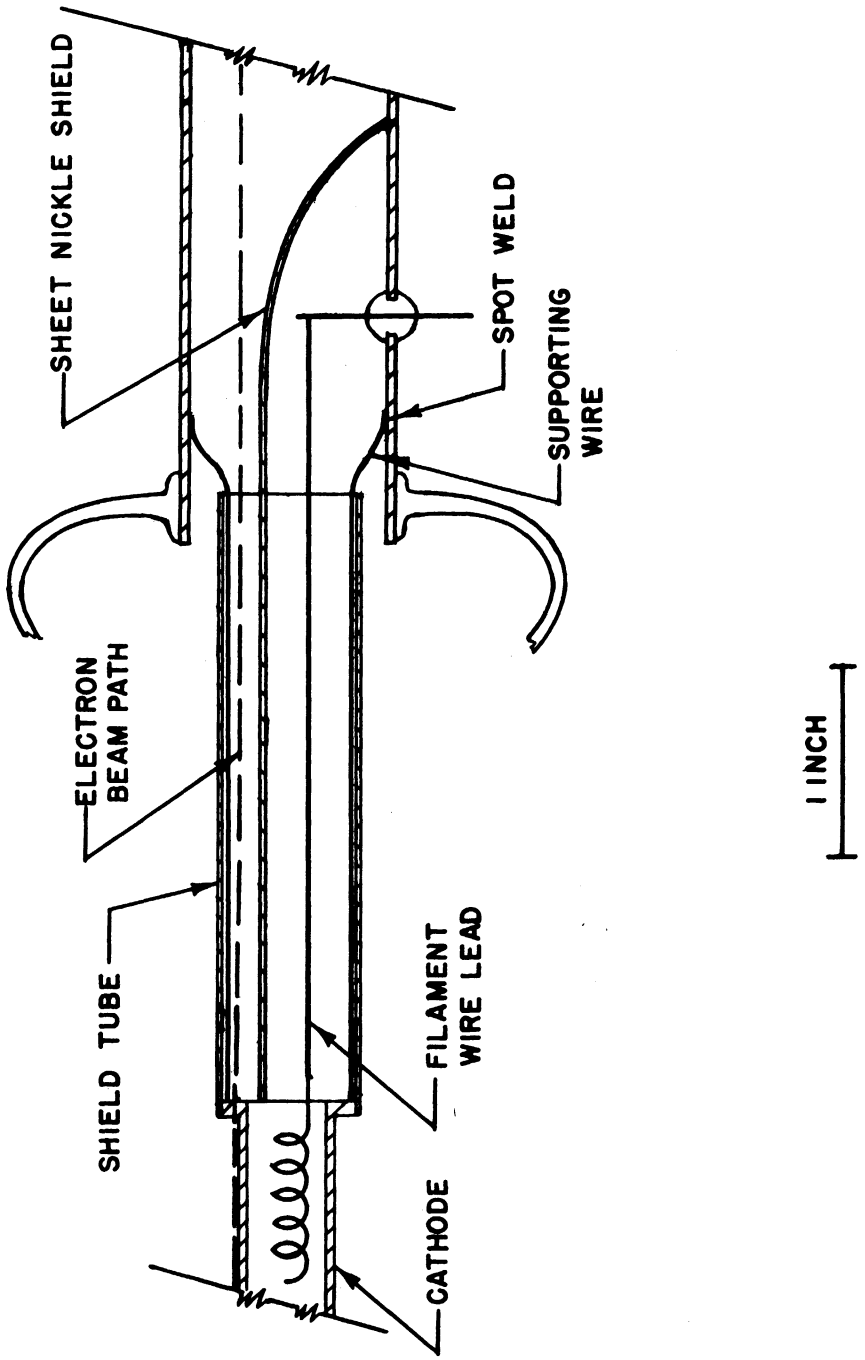

FIG. 9.4

ALL DIMENSIONS UNLESS OTHERWISE SPECIFIED MUST BE HELD TO A TOLERANCE - FRACTIONAL ± 1/64," DECIMAL ± .005," ANGULAR ± 1/2°

		ENGINEERING RESEARCH INSTITUTE UNIVERSITY OF MICHIGAN ANN ARBOR MICHIGAN	DESIGNED BY	APPROVED BY
			DRAWN BY nn	SCALE FULL
			CHECKED BY	DATE 9-21-50
		PROJECT M-762	TITLE CATHODE SUPPORT FOR TRAJECTRON	
		CLASSIFICATION	DWG. NO. A-11,004-1	
ISSUE	DATE			

of the fluorescent screen using a pen mounted in a compound tool rest. Thus these markings should be accurate within a few thousandths of an inch. The inside circle is the same diameter as the cathode, and the electron beam enters the space charge opposite the bottom intersection of the vertical line with this circle (Figure 9.2). The lines are made with a platinum paste, which will go through the bake-out. The photograph also shows where a small square of phosphor was removed from the screen to serve as a window for checking the cathode temperature.

The cooling coils and the assembly for cooling the fluorescent screen are not shown. It is hoped that the next report will show photographs of the tube in operation.

10. CONSTRUCTION OF MAGNETRONS

The tube construction phase of this period has been devoted to the construction of several tubes as well as to the development of new techniques for this laboratory.

A newly designed thoriated tungsten cathode was built and inserted in the Model 7A No. 33 magnetron (see section 4 of this report). It had a quarter wave length by-pass mounted on its stem in an attempt to eliminate the cathode coupling problem discussed in the Quarterly Progress Report No. 2. This cathode is shown in Figure 10.1. It was necessary to shorten the Kovar stem (part 11) to eliminate a heat problem due to conduction down the molybdenum by-pass (part 3).

A third 10-cm experimental magnetron diode was constructed (see section 5 of this report). It was designed to reduce the leakage current which occurred in the second model. Some difficulty was experienced in maintaining tension in the spring which keeps the filament taut. The tungsten spring would relieve itself of all tension at the bake out temperature of 420°C. The problem was solved by baking the tube out while on the pump without the cathode and then inserting the cathode followed by a bake out on the pumps at 200°C.

Construction was started on the low power insertion magnetron discussed in section 6. The original model 9 No. 35 developed a crack in the glass seal running between the inner and outer conductor while on the pump. Parts were machined for a new model of this tube, Model 9A, No. 38 and the tube is now partially assembled. The

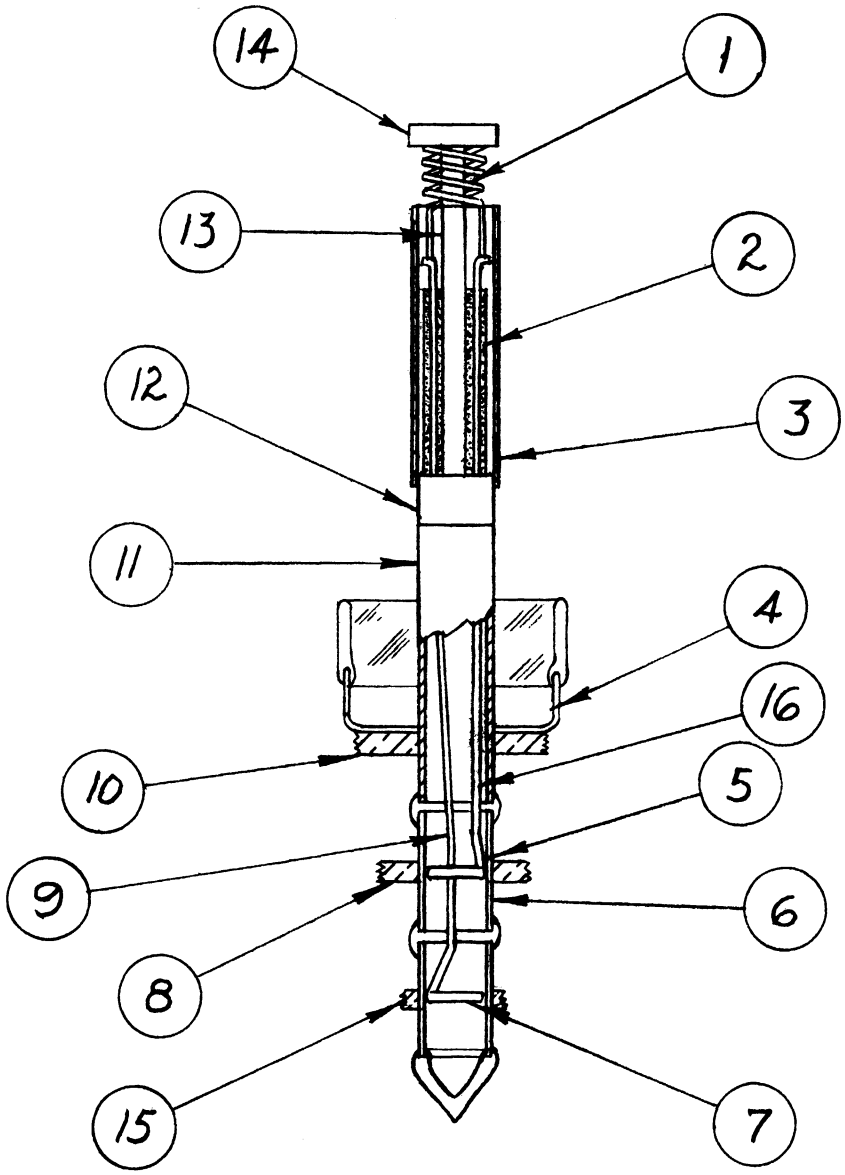

FIG. 10.1

ALL DIMENSIONS UNLESS OTHERWISE SPECIFIED MUST BE HELD TO A TOLERANCE - FRACTIONAL ± 1/64," DECIMAL ± .005," ANGULAR ± ½°

ENGINEERING RESEARCH INSTITUTE UNIVERSITY OF MICHIGAN ANN ARBOR MICHIGAN		DESIGNED BY J R B	APPROVED BY
		DRAWN BY N N	SCALE FULL
		CHECKED BY V R R	DATE 8-17-50
PROJECT M-762		TITLE TUNGSTEN CATHODE TUBE MODEL NO. 6, 7, 7A	
CLASSIFICATION		DWG. NO. A- 8012	
ISSUE	DATE		

new design incorporates an expansion joint in the inner conductor which will reduce strain on this seal. This tube should be completed in the near future.

Model 8, Tube No. 36 was completed in this period and is reported in section 8. Techniques new to this laboratory were employed in its construction. The glass seals between the cathodes and outer pole pieces were made by using a recently completed 20-KW induction heater. The cathodes were accurately aligned in the outer pole pieces by means of jigs while the seals were made. Later the outer pole pieces with their cathodes were silver-soldered to the inner pole pieces by means of the induction heater.

The trajectron, Model 11,004, Tube No. 37, was assembled in this period and is ready for the pumps. This tube is discussed in section 9. Since the tube is radical in design as compared to previous ones built in this laboratory, considerable experience was gained in construction techniques not used in earlier tubes. Among these may be listed large glass-to-metal seals, depositing fluorescent screens, constructing press seals, obtaining good adherence of oxide coating on large nickel surfaces, marking glass with a paint capable of withstanding high temperatures, etc. This tube should be off the pumps within a few days.

A 1.5-inch horizontal hydrogen furnace capable of 1600°C operation has been constructed in this period and will be used for firing tungsten filaments and for coating heaters.

11. CONCLUSIONS

Since all work in progress is in a state of partial completion, conclusions must be accepted as tentative. However, the progress during the period covered by this report may be summed up as follows:

(a) The results of analysis cannot be called positive but they do present quantitative answers which will be useful in conditioning future thinking. The validity of the simplified assumptions can be checked by comparing the numerical results, obtained in sections 2 and 3, with experimental observations. These results appear to indicate that well defined space charge spokes may not exist, and that transit time might place a limit on the maximum conduction current possible in the magnetron.

(b) Experimental study of the effects of emission and magnetic field on operation show a definite effect of cathode emission on starting voltage. The peculiar effects of magnetic field near the cyclotron resonance may be characteristic of this particular tube. They are, of course, very interesting but should not be taken too seriously in connection with the present study until more evidence is available.

(c) The study of r-f properties of the magnetron space charge is nearing completion (insofar as effort on this project is concerned). It seems to be possible to calculate correctly where (on the frequency scale) wave length shift will change in magnitude and sign. However, the calculation of loss and of magnitude of such shifts is still not always in good agreement

with experiment. This probably has a great deal to do with the difficulty of making the experimental tube produce exactly what is desired (because of nonuniformity in the structure or in the magnetic field).

(d) The construction of the "trajectron" tube for study of the static magnetron space charge and the insertion magnetron for use in an external cavity at low power levels has made satisfactory progress. The insertion magnetron, which is to be used for low Q studies, has been redesigned because of structural defects.

(e) The first Model 8 double anode magnetron has been completed and partially tested. The results prove the possibility of the operation of more than one set anode in the same cavity. No f-m data were taken.

(f) The study of modulation has been limited to the study of problems associated with the voltage tuning method. The development of the reactance tube method will be continued as soon as possible with the redesign of the Model 6 magnetron.

12. WORK IN PROSPECT

During the next quarterly period it will be necessary to spend considerable effort on preparation of final reports. These will take the form of three or four individual Technical Reports covering the topics of study which are sufficiently completed for an integrated report plus a final summary report surveying all progress on the contract. It is hoped that data will be available on the various magnetrons presently in construction, particularly in connection with low Q operation.

DISTRIBUTION LIST

22 copies - Director, Evans Signal Laboratory
Belmar, New Jersey
FOR - Chief, Thermionics Branch

12 copies - Chief, Bureau of Ships
Navy Department
Washington 25, D. C.
ATTENTION: Code 930A

12 copies - Director, Air Materiel Command
Wright Field
Dayton, Ohio
ATTENTION: Electron Tube Section

4 copies - Chief, Engineering and Technical Service
Office of the Chief Signal Officer
Washington 25, D. C.

2 copies - H. Wm. Welch, Jr., Research Physicist
Electron Tube Laboratory
Engineering Research Institute
University of Michigan
Ann Arbor, Michigan

1 copy - Engineering Research Institute File
University of Michigan
Ann Arbor, Michigan

W. E. Quinsey, Asst. to the Director
Engineering Research Institute
University of Michigan
Ann Arbor, Michigan

W. G. Dow, Professor
Dept. of Electrical Engineering
University of Michigan
Ann Arbor, Michigan

Gunnar Hok, Research Engineer
Engineering Research Institute
University of Michigan
Ann Arbor, Michigan

J. R. Black, Research Engineer
Engineering Research Institute
University of Michigan
Ann Arbor, Michigan

G. R. Brewer, Research Associate
Engineering Research Institute
University of Michigan
Ann Arbor, Michigan

J. S. Needle, Instructor
Dept. of Electrical Engineering
University of Michigan
Ann Arbor, Michigan

Dept. of Electrical Engineering
University of Minnesota
Minneapolis, Minnesota
ATTENTION: Prof. W. G. Shepherd

Westinghouse Engineering Laboratories
Bloomfield, New Jersey
ATTENTION: Dr. J. H. Findlay

Columbia Radiation Laboratory
Columbia University Dept. of Physics
New York 27, New York

Electron Tube Laboratory
Dept. of Electrical Engineering
University of Illinois
Urbana, Illinois

Dept. of Electrical Engineering
Stanford University
Stanford, California
ATTENTION: Dr. Karl Spangenberg

National Bureau of Standards Library
Room 203, Northwest Building
Washington 25, D. C.

Radio Corporation of America
RCA Laboratories Division
Princeton, New Jersey
ATTENTION: Mr. J. S. Donal, Jr.

Dept. of Electrical Engineering
The Pennsylvania State College
State College, Pennsylvania
ATTENTION: Prof. A. H. Waynick

Document Office - Room 20B-221
Research Laboratory of Electronics
Massachusetts Institute of Technology
Cambridge 39, Massachusetts
ATTENTION: John H. Hewitt

Bell Telephone Laboratories
Murray Hill, New Jersey
ATTENTION: S. Millman

Special Development Group
Lancaster Engineering Section
Radio Corporation of America
RCA Victor Division
Lancaster, Pennsylvania
ATTENTION: Hans K. Jenny

Magnetron Development Laboratory
Power Tube Division
Raytheon Manufacturing Company
Waltham 54, Massachusetts
ATTENTION: Edward C. Dench

Vacuum Tube Department
Federal Telecommunication Labs, Inc.
500 Washington Avenue
Nutley 10, New Jersey
ATTENTION: A. K. Wing, Jr.

Microwave Research Laboratory
University of California
Berkeley, California
ATTENTION: Prof. L. C. Marshall

General Electric Research Laboratory
Schenectady, New York
ATTENTION: Dr. Wilbur Hull

Cruft Laboratory
Harvard University
Cambridge, Massachusetts
ATTENTION: Prof. E. L. Chaffee

Research Laboratory of Electronics
Massachusetts Institute of Technology
Cambridge, Massachusetts
ATTENTION: Prof. S. T. Martin

Collins Radio Company
Cedar Rapids, Iowa
ATTENTION: Robert M. Mitchell

Dept. of Electrical Engineering
University of Kentucky
Lexington, Kentucky
ATTENTION: Prof. H. Alexander Romanowitz

Dept. of Electrical Engineering
Yale University
New Haven, Connecticut
ATTENTION: Dr. H. J. Reich

Department of Physics
Cornell University
Ithaca, New York
ATTENTION: Dr. L. P. Smith

Document Office for Government Research Contracts
Harvard University
Cambridge, Massachusetts
ATTENTION: Mrs. Marjorie L. Cox

Mr. R. E. Harrell
West Engineering Library
University of Michigan
Ann Arbor, Michigan

Mr. C. L. Cuccia
RCA Laboratories Division
Radio Corporation of America
Princeton, New Jersey

Dr. O. S. Duffendack, Director
Phillips Laboratories, Inc.
Irvington-on-Hudson, N. Y.